Table V. Independent factors associated with expression of $p33^{ING1}$

Factor	Stepwise multivariate analysis		
	Odds ratio	95% CI	*P* value
Differentiation			
1: WD	1		
2: MD & PD	8.19	2.03–30.2	0.0021
TNM stage			
1: I–II	1		
2: III–IV	3.4	1.21–8.01	0.0009

Abbreviations: CI = confidence interval; WD = well-differentiated; MD = moderately-differentiated; PD = poorly differentiated.

cyclin E kinase activity in HCC with nuclear staining tended to be lower than that in HCC with cytoplasmic $p33^{ING1}$ staining. Spearman correlation coefficients were used to evaluate whether $p33^{ING1}$ expression in HCC correlated with cyclin E kinase activity and certain clinicopathological variables. Loss of $p33^{ING1}$ expression correlated with greater cyclin E kinase activity (Spearman $r = 0.81$, $n = 29$, $P = 0.0001$), poorer histological differentiation (Spearman $r = 0.59$, $n = 29$, $P = 0.0008$) and advanced TNM stage (Spearman $r = 0.40$, $n = 29$, $P = 0.030$). The most significant correlate of decreased $p33^{ING1}$ expression in patients with HCC was increased cyclin E kinase activity.

Western blot of cyclin E in HCC

The cyclin E immunoreactive band was seen on Western blots at the molecular size of 50 kDa. Although the difference of the protein level of cyclin E in HCC was small as compared with the difference of cyclin E kinase activity, the level of cyclin E kinase activity appeared to correlate with the amount of cyclin E (Fig. 3B and D).

Discussion

The major finding of the present study was reduced expression of $p33^{ING1}$ in HCC, especially in moderately and poorly differentiated tumours. In contrast, abundant $p33^{ING1}$ expression was detected in the hepatocellular nuclei in normal liver, chronic hepatitis (F1, F2 and F3) and liver cirrhosis (F4), as well as in well-differentiated HCC. In subsets of cases of liver

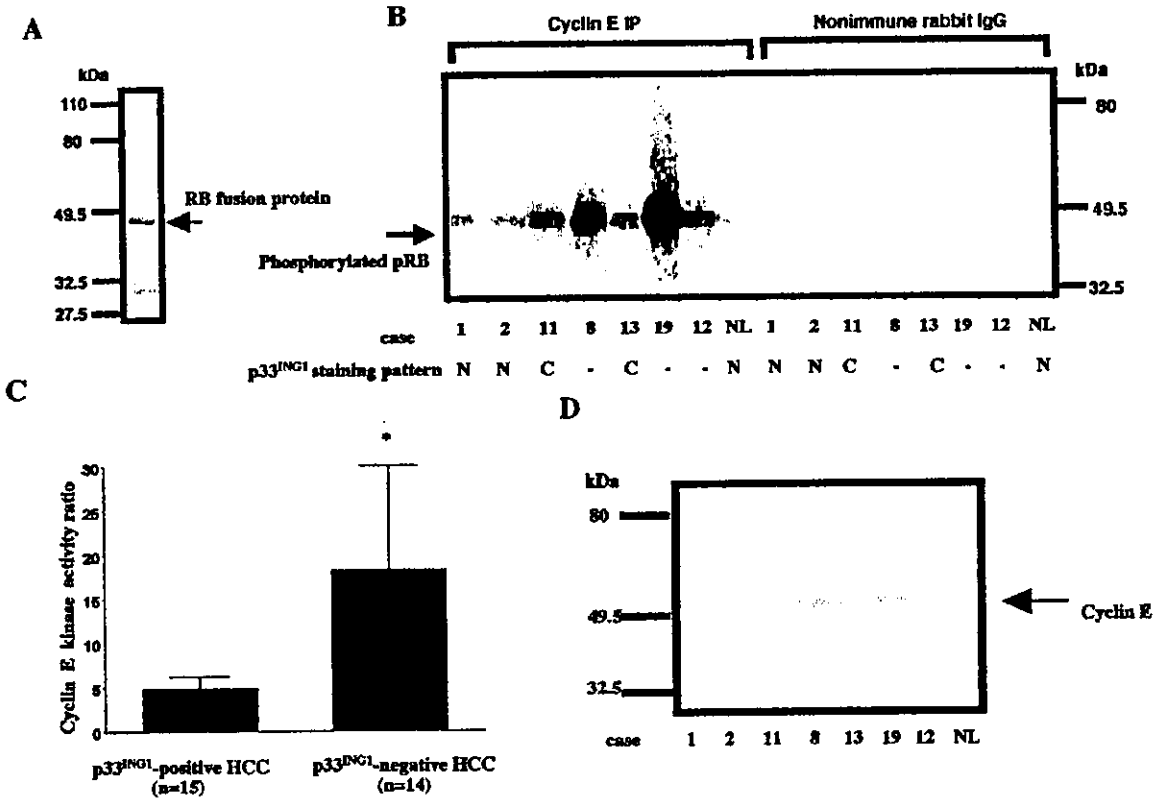

Fig. 3. A. Sodium dodecyl sulphate-polyacrylamid e gel electrophoresi s (SDS-PAGE) profile of a glutathione S-transferase (GST)-Rb fusion protein. Staining showed a single band of 46 kDa (arrow). B. Phosphorylation patterns of pRb as shown by immunostaining of $p33^{ING1}$ in tumour sections, with staining indicated as N, nuclear; C, cytoplasmic; or –, negative. Cyclin E-immunoprecipitated samples from tumour lysates were used in this cyclin E kinase assay. Radioactivity in the phosphorylated Rb band is shown by an arrow. In HCC cases in which $p33^{ING1}$ was not expressed, the cyclin E kinase activity was high. In contrast, the cyclin E kinase activity in HCC with high $p33^{ING1}$ expression (especially in HCC cases with a nuclear staining pattern) was very low. Case numbers correspond to those in Table III. C. Tumour (T)-to-normal liver (N) ratios of cyclin E kinase activity in $p33^{ING1}$-negative HCC ($n = 14$) and $p33^{ING1}$-positive HCC ($n = 15$). Values represent the mean ± *s* (SD). Cyclin E kinase activity in $p33^{ING1}$-negative HCC was significantly higher than that in $p33^{ING1}$-positive HCC ($P = 0.001$, Student's *t* test). D. Western blot of cyclin E in tumour lysates. The cyclin E immunoreactive band was seen at the molecular size of 50 kDa, and the amount of cyclin E correlated with the level of cyclin E kinase.

cirrhosis (F4) and HCC, expression of $p33^{ING1}$ was detected in the cytoplasm of hepatocytes and/or cancer cells. Furthermore, loss of $p33^{ING1}$ does not usually occur in normal liver, chronic hepatitis, liver cirrhosis or well-differentiated HCC, but does occur in moderately or poorly differentiated HCC and in advanced-stage HCC. It is therefore considered that loss of $p33^{ING1}$ expression occurs as a late event in hepatocarcinogenesis.

The *ING1* gene has been mapped to chromosome 13 at the q33 to q34 region, where chromosomal translocation or deletion has frequently been found in various human cancers including HCC (9–11). Such an event might explain the loss of $p33^{ING1}$ expression in a subset of HCC that was found in this study. A marked decrease of $p33^{ING1}$ expression has been observed in breast (15, 16), gastric (12), head and neck cancers (14), and also in malignant lymphoma (13). In addition, in vitro experiments indicate that inhibition of $p33^{ING1}$ expression increases the frequency of proliferative locus formation in NIH3T3 cells and prolongs the life span of diploid fibroblasts in culture (6). Decreased $p33^{ING1}$ expression may generally be involved in malignant transformation, as suggested by the correlations deserved in the present study of HCC.

To date, $p33^{ING1}$ has not been found to regulate cell differentiation. To investigate the possible involvement of this protein in the differentiation of HCC, we analysed the relationship between the level of $p33^{ING1}$ expression and the histological grade of HCC. Expression of $p33^{ING1}$ was reduced in moderately and poorly differentiated HCC compared to well-differentiated HCC. These data suggest that decreased expression of $p33^{ING1}$ may be important in the dedifferentiation of HCC in addition to malignant transformation leading to HCC. However, our results did not directly prove or explain the involvement of $p33^{ING1}$ in promoting or inhibiting differentiation of hepatic cancer cells. In addition, in immunohistochemical analyses of $p33^{ING1}$, we noted an inverse correlation between $p33^{ING1}$ expression and tumour aggressiveness as indicated by TNM classification. Our results demonstrated that loss of $p33^{ING1}$ was particularly evident in advanced HCC (stages III and IV), suggesting that decreased $p33^{ING1}$ may somehow promote progression of HCC.

To elucidate the possible mechanisms of the reduction of $p33^{ING1}$ protein in HCC, we carried out PCR-SSCP and direct sequencing of the *ING1* gene. No point mutations or deletions were found in 5 poorly differentiated HCCs or 2 moderately differentiated HCCs with significantly decreased $p33^{ING1}$ expression (data not shown). These data suggest that mutation of $p33^{ING1}$ is rare in HCC. Since decreased $p33^{ING1}$ expression frequently accompanies HCC development, mechanisms such as homozygous deletion or hypermethylation of the *ING1* gene may be responsible for reduced $p33^{ING1}$ expression. Further studies will be required to explore these possibilities.

The $p33^{ING1}$ protein has been shown to activate the $p21^{WAF1}$ promoter (7). This fact suggests that $p33^{ING1}$ may down-regulate the activity of cell-cycle-related kinases, such as cyclins E, D, A or B. Regarding these cyclins we previously found increased cyclin E kinase activity was particularly important in hepatic tumour development in an animal HCC model, the Long-Evans Cinnamon (LEC) rat (26). Therefore, to determine whether reduced $p33^{ING1}$ expression in HCC cells is related to increased cell proliferation, we analysed cyclin E kinase activity, a well-established G1 phase-specific proliferative marker (17). Cyclin E kinase activity was increased in HCC with loss of $p33^{ING1}$, underscoring the functional importance of loss of $p33^{ING1}$ in HCC. Reduced $p33^{ING1}$ may be one of several factors contributing to malignant transformation, progression and differentiation occurring via up-regulation of cyclin E kinase activity.

In conclusion, we found that loss of $p33^{ING1}$ protein was frequent in HCC, especially in moderately and poorly differentiated tumours as well as in aggressive and advanced lesions. Loss of $p33^{ING1}$ may be important in the process of malignant transformation, and appears to be closely related to histological differentiation of HCC. In addition, loss of $p33^{ING1}$ was shown to be associated with up-regulation of cyclin E kinase activity, a proliferative marker. In the future, novel therapeutic strategies aiming to enhance $p33^{ING1}$ expression may be useful for preventing the development and progression of HCC.

Acknowledgements

We thank Dr. K. Riabowol (University of Calgary) for the gift of the $p33^{ING1}$ antibody. This work was supported in part by a Grant-in-Aid for Scientific Research (B-14370185) from the Japanese Ministry of Education, Sciences Sports and Culture of Japan.

References

1. Naka T, Toyota N, Kaneko T, Kaibara N. Protein expression of p53, p21WAF1, and Rb as prognostic indicators in patients with surgically treated hepatocellular carcinoma. Anticancer Res 1998;18:555–64.
2. Levine AJ. p53, the cellular gatekeeper for growth and division. Cell 1997;88:323–31.
3. Garkavtsev I, Kazarov A, Gudkov A, Riabowol K. Suppression of the novel growth inhibitor p33ING1 promotes neoplastic transformation. Nature Genet 1996;14:415–20.
4. Shimada Y, Saito A, Suzuki M, Takahashi E, Horie M. Cloning of a novel gene (ING1L) homologous to ING 1, a candidate tumor suppressor. Cytogenet Cell Genet 1998;83:232–5.
5. Garkavtsev I, Grigorian IA, Ossovskaya VS, Chernov MV, Chumakov PM, Gudkov AV. The candidate tumor suppressor p33ING1 cooperates with p53 in cell growth control. Nature 1998;391:295–8.
6. Helbing CC, Veillette C, Riabowol K, Johnston RN, Garkavtsev I. A novel candidate tumor suppressor, ING1, is involved in the regulation of apoptosis. Cancer Res 1997;57:1255–8.
7. Garkavtsev I, Boland D, Mai J, Wilson H, Veillete C, Riabowol K. Specific monoclonal antibody raised against the p33ING1 tumor suppressor. Hybridoma 1997;16:537–40.
8. Zeremski M, Horrigan, SK, Grigorian, IA, Westbrook CA,

Gudkov AV. Localization of the candidate tumor suppressor gene ING1 to human chromosome 13q34. Somat Cell Molec Genet 1997:23:233–6.
9. Maestro R, Piccinin S, Doglionic C, Gasparotto D, Vukosavljevic T, Sulfaro S, et al. Chromosome 13q delation mapping in head and neck squamous cell carcinomas: identification of two distant regions of preferential loss. Cancer Res 1996;56:1146–50.
10. Motomura K, Nishisho I, Takai S, Tateishi H, Okazaki M, Takai S. Loss of alleles at loci on chromosome 13 in human primary gastric cancers. Genomics 1998;2:180–4.
11. Nishida N, Fukuda Y, Kokuryu H, Sadamoto T, Isowa G, Honda K, et al. Accumulation of allelic loss on arms of chromosomes 13q, 16q and 17q in the advanced stages of human hepatocellular carcinoma. Int J Cancer 1992;51:862–8.
12. Oki E, Maehara Y, Tokunaga E, Kakeji Y, Sugimachi K. Reduced expression of p33(ING1) and the relationship with p53 expression in human gastric cancer. Cancer Lett 1999;147:157–62.
13. Ohmori M, Nagai M, Tasaka T, Koeffler HP, Riabowol K, Takahara J. Decreased expression of p33ING1 mRNA in lymphoid malignancies. Am J Hematol 1999;62:118–9.
14. Sanchez-Cespede M, Okami K, Cairns P, Sidransky D. Molecular analysis of candidate tumor suppressor gene ING1 in human head and neck tumors with 13q deletions. Genes Chromosomes Cancer 2000;27:319–22.
15. Tokunaga E, Maehara Y, Oki E, Kitamura K, Kakeji Y, Ohno S, et al. Diminished expression of ING1 mRNA and the correlation with p53 expression in breast cancers. Cancer Lett 2000;152:15–22.
16. Toyama T, Iwase H, Watson P, Muzik H, Saettler E, Magliocco A, et al. Suppression of ING1 expression in sporadic breast cancer. Oncogene 1999;18:5187–93.
17. Hunter T, Pines J. Cyclins and cancer II: cyclin D and CDK inhibitors come of age. Cell 1994;79:573–82.
18. International Working Party. Terminology of nodular hepatocellular lesions. Hepatology 1995;22:983–93.
19. Desmet VJ, Gerber M, Hoofnagle JH, Manns M, Scheuer PJ. Classification of chronic hepatitis: diagnosis, grading and staging. Hepatology 1994;19:1513–20.
20. Hsu SM, Raine L, Fangen H. Use of avidine-biotin-peroxidase complex (ABC) in immunoperoxidase techniques: a comparison between ABC and unlabeled antibody (PAP) procedures. J Histochem Cytochem 1981;29:577–80.
21. Hunyady B, Krempels K, Harta G, Mezey E. Immunohistochemical signal amplification by catalyzed reporter deposition and its application in double immunostaining. Histochem Cytochem 1996;44:1353–62.
22. Matsushime H, Ewen ME, Strom DK, Kato J, Hanks SK, Roussel MF, et al. Identification and properties of an atypical catalytic subunit (p34PSKJ3/cdk4) for mammalian D type G1 cyclins. Cell 1992;71:323–34.
23. Matsushime H, Roussel MF, Ashmun RA, Sherr CJ. Colony-stimulating factor 1 regulates novel cyclins during the G1 phase of the cell cycle. Cell 1991;65:701–13.
24. Laemmli UK. Cleavage of structural proteins during the assembly of the head of bacteriophage T4. Nature 1970;227:680–5.
25. Towbin H, Stadhelin T, Gordon J. Electrophoretic transfer of proteins from polyacrylamide gel to nitrocellulose sheets: procedure and some application. Proc Natl Acad Sci USA 1979;76:4350–4.
26. Masaki T, Shiratori Y, Rengifo W, Igarashi K, Matsumoto K, Nishioka M, et al. Hepatocellular carcinoma cell cycle: study of LEC rat. Hepatology 2000;32:711–20.
27. Bradford MM. A rapid and sensitive method for the quantitation of microgram quantities of protein utilizing the principle of protein-dye binding. Analytical Biochem 1976;72:248–54.

Received 26 April 2002
Accepted 18 September 2002

Tissue Inhibitor of Metalloproteinases-1 Attenuates Spontaneous Liver Fibrosis Resolution in the Transgenic Mouse

Hitoshi Yoshiji,[1] Shigeki Kuriyama,[2] Junichi Yoshii,[1] Yasuhide Ikenaka,[1] Ryuichi Noguchi,[1] Toshiya Nakatani,[1] Hirohisa Tsujinoue,[1] Koji Yanase,[1] Tadashi Namisaki,[1] Hiroo Imazu,[1] and Hiroshi Fukui[1]

It has been suggested that the tissue inhibitor of metalloproteinases-1 (TIMP-1) is involved in spontaneous resolution of liver fibrosis. The aim of this study was to investigate whether TIMP-1 altered spontaneous resolution of liver fibrosis in conjunction with matrix metalloproteinases (MMP) inhibition and hepatic stellate cell (HSC) activation. The livers of liver-targeted TIMP-1 transgenic (TIMP-Tg) and control hybrid (Cont) mice were harvested at 0, 3, 7, and 28 days following spontaneous recovery from CCl_4-induced liver fibrosis. The extent of fibrosis resolution, MMP expression, α-smooth-muscle actin (α-SMA) positive cells, and procollagen-(I) messenger RNA (mRNA) in the liver were assessed at the respective periods in both groups. We also examined the effect of TIMP-1 on HSC apoptosis. The TIMP-Tg mice showed significantly attenuated resolution of spontaneous liver fibrosis compared with the Cont mice. The hydroxyproline content, number of α-SMA positive cells, and procollagen-(I) mRNA rapidly decreased with time in the Cont mice, whereas these markers were little changed in TIMP-Tg mice. The level of the active form of metalloproteinases-2 (MMP-2) in the TIMP-Tg mice was less than that in the Cont mice. TIMP-1 markedly decreased the nonparenchyma apoptotic cells in the liver fibrosis resolution model, and it also inhibited HSC apoptosis associated with suppression of caspase-3 activity *in vitro*. In conclusion, TIMP-1 significantly attenuated spontaneous resolution of liver fibrosis by the combination of a net reduction of the MMP activity and suppression of apoptosis in HSC. (HEPATOLOGY 2002;36:850-860.)

Liver fibrosis is the result of alteration of the extracellular matrix (ECM), which consists of fibrin-forming collagens, especially collagen type-I, and other matrix components such as proteoglycans, fibronectins, and hyaluronic acid.[1-3] It has been considered that the advanced fibrotic change is irreversible even after withdrawal of the liver-injuring agent.[4] Fibrosis, however, now can be regarded as a dynamic and potentially reversible process. In animal experiments, the reversibility of liver fibrosis has been shown in several experimental models using chronic carbon tetrachloride (CCl_4), thioacetamide, and bile duct ligation. Even in the clinical practice, several reports have suggested that fibrosis development in chronic liver injury may be reversed, *e.g.*, in interferon-treated chronic viral hepatitis.[4,5]

Regardless of the etiologic factors, gross remodeling of ECM in the fibrotic liver is regulated by a balance of synthesis and enzymatic degradation of ECM.[2,3] Matrix degradation is catalyzed by the activity of matrix metalloproteinases (MMPs), which consist of collagenases, gelatinases, stromelysins, and membrane type (MT)-MMPs. The activities of MMPs are inhibited by tissue inhibitors of metalloproteinases (TIMPs) because of formation of a noncovalent 1:1 complex with the MMPs.[6] Because the predominant collagens in the fibrotic liver are collagen type I and III, the expression of the interstitial collagenase (MMP-1) activity would be necessary to initiate collagen

Abbreviations: ECM, extracellular matrix; MMP, matrix metalloproteinases; TIMP-1, tissue inhibitor of metalloproteinases-1; α-SMA, α-smooth-muscle actin; HSC, hepatic stellate cell.

From the [1]Third Department of Internal Medicine, Nara Medical University, Nara; and [2]Third Department of Internal Medicine, Kagawa Medical University, Kagawa, Japan.

Received January 16, 2002; accepted July 1, 2002.

Supported in part by a grant in aid for scientific research (C-14570498) from the Japanese Ministry of Education, Sciences, Sports, and Culture.

Address reprint requests to: Hitoshi Yoshiji, M.D., Ph.D., Third Department of Internal Medicine, Nara Medical University, Shijo-cho 840, Kashihara, Nara 634-8522, Japan. E-mail: yoshijih@naramed-u.ac.jp; fax: (81) 744-24-7122.

0270-9139/02/3604-0010$35.00/0

doi:10.1053/jhep.2002.35625

degradation. Although the alteration of MMP-1 is still controversial, recent studies have suggested that gene expression of MMP-1 or the rat homologue of interstitial collagenase (MMP-13) relatively persisted during ECM remodeling in liver fibrosis development and resolution. On the other hand, the expression of TIMPs drastically increased or decreased with time during liver fibrogenesis and fibrosis resolution, respectively.[7-15] Four members of the TIMP family have been characterized so far and designated as TIMP-1 to TIMP-4.[6] In the liver, TIMP-1 and TIMP-2 were identified, and it has been suggested that TIMP-1 plays a more important role in the pathogenesis of liver fibrosis than TIMP-2.[13-15] During the development of liver fibrosis in the experimental models and human samples, TIMP-1 expression has been shown to be significantly increased in both the liver and the serum. The liver TIMP-1 protein levels also closely correlated with the histologic degree of liver fibrosis.[8-11,16-19] We previously reported that overexpression of TIMP-1 significantly promoted experimental liver fibrogenesis.[20] On the contrary, the TIMP-1 expression level rapidly decreased during spontaneous liver fibrosis resolution in the experimental model, and this alteration was associated with a marked increase in hepatic stellate cells (HSC) apoptosis, which plays an important role in the pathogenesis of liver fibrosis.[7,13,14] These results suggested that apoptosis of the activated HSC may virtually contribute to resolution of liver fibrosis in conjunction with the decrease in TIMP-1 expression. TIMP-1 has been shown to inhibit apoptosis in several types of cells, and this effect is sometimes independent of MMP inhibition.[6,21-24] Very recently, it has been shown that TIMP-1 inhibits apoptosis in the activated HSC through MMP inhibition *in vitro*.[25] Accordingly, it is likely that TIMP-1 inhibits resolution of liver fibrosis through prevention of HSC apoptosis. To address this issue, in the present study, we employed the liver-targeted TIMP-1 transgenic (TIMP-Tg) mouse model, which can achieve a high TIMP-1 level in the liver microenvironment, to examine the effect of overexpression of TIMP-1 on the spontaneous resolution of liver fibrosis. We also examined the possible interactions between HSC apoptosis and TIMP-1.

Materials and Methods

Animals. The details of the liver-targeted TIMP-Tg mouse model have been described previously.[20] Briefly, mouse albumin enhancer/promoter was used to target the liver expression of TIMP-1. Because TIMP-1 possesses a secretion signal sequence, high levels of TIMP-1 can be detected in both the liver and the serum. The biologic activity of TIMP-1 in the TIMP-Tg mice measured by reverse zymography was 3.4-fold higher than that of the C57BL/6J-CBA control hybrid (Cont) mice. To develop liver fibrosis, each mouse received an intraperitoneal injection of CCl_4 (1 mg/kg/body weight) twice a week in a 1:1 ratio with corn oil. Because we previously reported that the TIMP-Tg mice showed promotion of CCl_4-induced liver fibrosis development more than the Cont mice,[20] we performed the following preliminary study. The fibrosis extension after the same period of CCl_4 treatment was quite different between the TIMP-Tg mice and Cont mice. We therefore compared the fibrosis extension in the TIMP-Tg mice and Cont mice after 4- to 10-week CCl_4 treatment. We found that a similar level of fibrosis development was achieved in the TIMP-Tg mice and Cont mice after 4- and 9-week treatment, respectively. In addition to the morphologic evaluation, we compared the hydroxyproline content, serum hyaluronic acid, and TGF-β level in the liver. All these markers were also at comparable levels in both groups. Accordingly, we injected CCl_4 into the TIMP-Tg and Cont mice for 4 and 9 weeks, respectively, in the present study ($n = 20$ for each group). The peak fibrotic change was noticed on the third day after the last injection, and this was designated as day 0.[7] We also examined the corn oil-treated animals in the TIMP-Tg and Cont groups. As previously reported,[20] neither gross nor microscopic abnormalities in the liver, including fibrosis development or ECM remodeling, were observed in the corn oil-treated animals in the TIMP-Tg and Cont groups (data not shown). During the spontaneous resolution period, 5 mice from each group were killed on days 0, 3, 7, and 28, respectively, under ether anesthesia. All animal procedures were performed according to the recommendations for the proper care and use of laboratory animals.

Histopathologic and Immunohistochemical Examinations. Five-micrometer-thick sections of formalin-fixed and paraffin-embedded livers were processed routinely for hematoxylin and eosin and Azan-Mallory staining. Immunohistochemical staining of α-SMA (DAKO, Kyoto, Japan) and apoptotic cell detection with the DNA fragmentation products that were stained by *in situ* 3′-end labeling (terminal deoxynucleotidyl transferase-mediated dUTP nick labeling [TUNEL]) were performed with paraffin-embedded sections as previously described.[20,26] Quantitative analysis of fibrosis development and measurement of the immunopositive cell area were carried out with the Fuji-BAS 2000 image analyzing

system (Fuji, Tokyo, Japan) in 6 microscopic fields (40× magnification) of specimens taken from 5 mice as described previously.[20,27] We did not count the α-SMA positive vessels in the portal area, which were assumed to be hepatic arteries. We only included α-SMA positive cells in the sinusoidal lining for image analysis.

Hepatic Hydroxyproline Content. The 200-mg frozen samples obtained at each time point were hydrolyzed in 6 mol/L HCl and analyzed for the total hydroxyproline content as described previously.[20,27] Briefly, the liver specimens were weighed, and 200 mg of frozen samples were hydrolyzed in 6 mol/L HCl in an autoclave for 24 hours. After centrifugation, the supernatant was mixed with 1% phenolphthalein and 8 N KOH to obtain a liquid at pH 7-8. This solution was stirred with KCl and borate buffer (pH 8.2) for 15 minutes at room temperature and for another 15 minutes at 0°C. Then, chloramine T solution was added and stirred for 60 minutes at 0°C. After addition of 3.6 mol/L sodium thiosulfate, the solution was incubated for 30 minutes at 120°C and stirred with a toluene for 20 minutes. Then, Ehrlich's solution was added to the supernatant after centrifugation at 2,000 rpm at 4°C and left for 30 minutes at room temperature. The absorbance was measured at 560 nm. The hydroxyproline content was expressed as μg/g wet liver.

TIMP-1 Biologic Activity and MMP-2 Level in the Liver. The liver lysates, which had equalized protein concentrations, were prepared as described previously.[20] The TIMP-1 biologic activity, which was measured by the MMP inhibitory activity, was assessed by reverse zymography. MMP-2 was used as a source of gelatinolytic activity at a concentration of 160 ng/mL. Although it was not possible to differentiate between the human and the endogenous mouse TIMP-1 by this method, the net MMP inhibitory activity, corresponding to TIMP-1, could be assessed semiquantitatively by densitometric analysis of the zymographs. The MMP-2 level was measured by an ELISA detection kit (Biotrak; Amercham Pharmacia Biotech, Tokyo, Japan) according to the manufacturer's instructions. This kit can measure both the active and total (pro and active) forms of MMP-2 with or without p-aminophenylmercuric acetate (APMA) treatment for activation. We measured both forms in each sample in triplicate (n = 5). Because the ELISA kit for MMP-13 was not available, we measured MMP-13 expression by real-time PCR.

The RNA Expressions of MMP-13 and Procollagen-(I) by Real-Time PCR. The MMP-13 and procollagen-(I) messenger RNA (mRNA) expressions were evaluated by real-time PCR as described previously.[27,28] The mRNA was extracted from 5 mice of each group at the respective killing periods. For cDNA synthesis, Taqman reverse transcription reagents were used as described in the manufacturer's manual of the ABI Prism 7700 Sequence Detection System (PE Applied Biosystems, Foster City, CA), which was used for real-time PCR amplification following the Taqman Universal PCR Master Mix Protocol (PE Applied Biosystems). Relative quantification of gene expression was performed as described in the manual, using glyceraldehyde-3-phosphate dehydrogenase (GAPDH) as an internal control. The threshold cycle and the standard curve method were used for calculating the relative amount of the target RNA as described by PE. The following temperature levels were employed: hold 50°C for 2 minutes, hold 60°C for 30 minutes, hold 94°C for 5 minutes, cycle 45 repeats 94°C for 1 minute, 55°C for 1 minute, and 72°C for 1 minute. To prevent genomic DNA contamination, all RNA samples were subjected to DNase I digestion and were checked by 40 cycles of PCR to confirm the absence of amplified DNA.

Isolation and Culture of HSC. We tried several times to isolate the pure HSC from the liver of mice; however, we found that we could not rule out the contamination of other types of nonparenchyma cells, such as endothelial cells. Also, the yield of purified HSC from the mouse was very low to perform several experiments as described previously.[20,29] We thus employed the HSC from the liver of rats to examine the effect of TIMP-1 on HSC apoptosis *in vitro*.

After 5-day culture, HSC became myofibroblast like, with reduced lipid vesicles and increased immunoreactive α-SMA, and, after 7-day plating, all the cells were well spread and α-SMA positive.[29] On day 10, HSC apoptosis was induced by serum-free conditions as described elsewhere,[25] either with or without recombinant human TIMP-1 (rTIMP-1; Fuji Chemical, Toyama, Japan) at doses of 50 and 500 ng/mL. Twelve hours after the incubation, the HSC apoptosis was detected by the Cell Death Detection ELISA kit (Roche, Tokyo, Japan) and Apop-Ladder Ex kit (Takara, Kyoto, Japan) according to the respective manufacturer's instructions. The caspase-3 activity was measured by the ApoAlart caspase colorimetric assay kits according to the manufacturer's instructions (Clontech, Tokyo, Japan).

Statistical Analysis. To assess the statistical significance of intergroup differences in the quantitative data, Bonferroni's multiple comparison test was performed after 1-way analysis of variance (ANOVA), followed by Bartlett's test to determine the homology of variance.

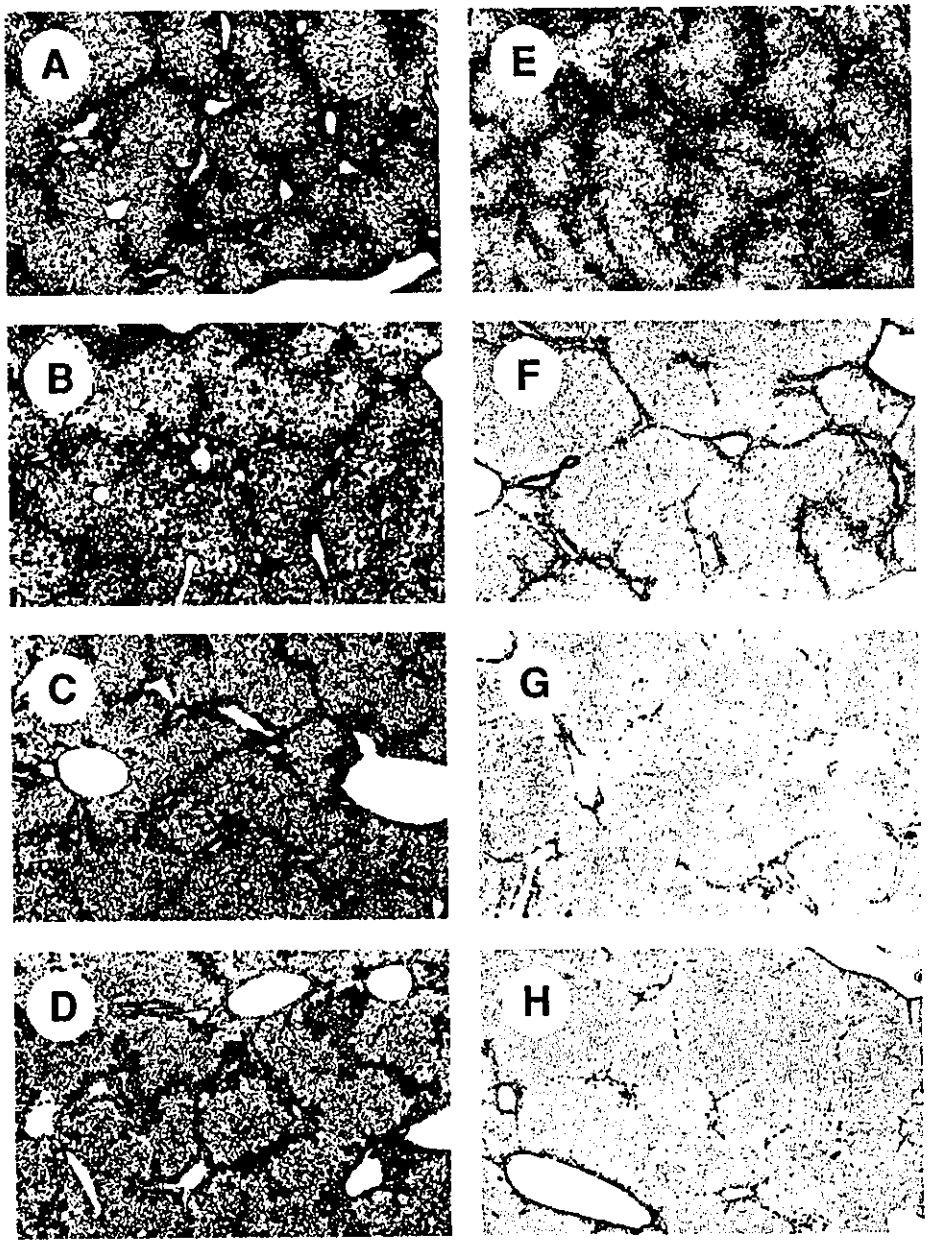

Fig. 1. Photomicrographs of liver sections during spontaneous fibrosis resolution. The TIMP-Tg mice and Cont mice received CCl_4 treatment for 4 and 9 weeks, respectively. The sections from TIMP-Tg mice and Cont mice were taken on day 0 (TIMP: A, Cont: E), day 3 (TIMP: B, Cont: F), day 7 (TIMP: C, Cont: G), and day 28 (TIMP: D, Cont: H). Spontaneous liver fibrosis resolution was already apparently observed by day 3 in the Cont mice, whereas resolution was significantly suppressed in the TIMP-Tg mice (Azan-Mallory stain, original magnification ×40).

Results

Effect of TIMP-1 on Spontaneous Liver Fibrosis Resolution. After 4 weeks and 9 weeks of CCl_4 injection, Azan-Mallory staining and densitometric analysis revealed similar fibrosis development in the TIMP-Tg mice and Cont mice, respectively. A similar level of dense fibrotic septum development with nodule formation was found in both groups on day 0 (Fig. 1A: TIMP-Tg mice, Fig. 1E: Cont mice). In accordance with previous reports,[7,12,30-32] a marked spontaneous liver fibrosis resolution was observed with time in the Cont mice after cessation of CCl_4 treatment (Fig. 1E-H). Spontaneous liver fibrosis resolution was already apparently observed by day 3 in the Cont mice (Fig. 1F). As shown in Fig. 1G, the liver histology appeared to be much closer to the normal histology with less fibrotic septa on day 7. Twenty-eight days after the peak fibrosis, most of the fibrotic septa were resolved, and small, little fibrotic fragments could be found (Fig. 1H). On the other hand, this spontaneous liver fibrosis resolution was significantly attenuated in the TIMP-Tg mice. No remarkable liver fibrosis resolution was found on days 3 and 7 (Fig. 1B and C, respectively). Even by day 28, marked fibrotic septa and nodule forma-

tion were still observed (Fig. 1D). Densitometric analysis of the fibrotic area and the hepatic hydroxyproline content confirmed the histologic changes. As shown in Fig. 2A, significant reductions of the fibrotic area and the hydroxyproline content were found on day 3 in the Cont mice as compared with the TIMP-Tg mice ($P < .01$). On the other hand, no significant differences in both markers were observed in the TIMP-Tg mice even on day 28 during the experiment. The TIMP-1 activity in the liver rapidly decreased with time in the Cont mice, whereas only a slight decrease could be found in the TIMP-Tg mice during the experiment (Fig. 2C). The reductions of the fibrotic area and the hepatic hydroxyproline content showed a similar pattern to that of the TIMP-1 activity reduction.

MMP-2 and MMP-13 Expression in the Liver. Because it has been shown that the net balance between MMPs and TIMP-1 plays an important role in ECM remodeling, we measured the MMP-2 and MMP-13 expression levels. In accordance with previous reports,[31,32] the MMP-2 level decreased with time in both the TIMP-Tg mice and Cont mice. Although the total MMP-2 level was higher in the TIMP-Tg mice than in the Cont mice because of the transgenic TIMP-1, the active form of MMP-2 was significantly lower in the TIMP-Tg mice than in the Cont mice at the respective periods (Fig. 3A and B). In the current study, the MMP-13 mRNA expression was not markedly altered during the experiment in both the TIMP-Tg mice and Cont mice (Fig. 3C). We also found that the serum ALT and total bilirubin levels in the TIMP-Tg mice were not different from those in the Cont mice on day 0, indicating that CCl_4 intoxication *per se* did not alter the liver dysfunction as previously described.[20] This suggests that attenuation of spontaneous resolution of liver fibrosis by TIMP-1 was not a secondary nonspecific cytoprotective effect of the transgenic TIMP-1 (data not shown).

Effect of TIMP-1 on HSC Activation in the Liver. Immunohistochemical analysis of α-SMA was carried out to examine the effect of TIMP-1 on HSC activation during spontaneous resolution of liver fibrosis. Similar to the histologic findings, the α-SMA positive cells were significantly decreased during spontaneous liver fibrosis resolution in the Cont mice (Fig. 4E-H). Even on day 3, the α-SMA positive cells were significantly decreased, which could be observed in clusters around the fibrotic septa (Fig. 4F). On day 28, only scattered α-SMA positive cells were found in the liver of the Cont mice (Fig. 4H). On the contrary, there were no marked differences in the number of α-SMA immunopositive cells in the liver of the TIMP-Tg mice from day 0 to day 28 (Fig. 4A-D). Com-

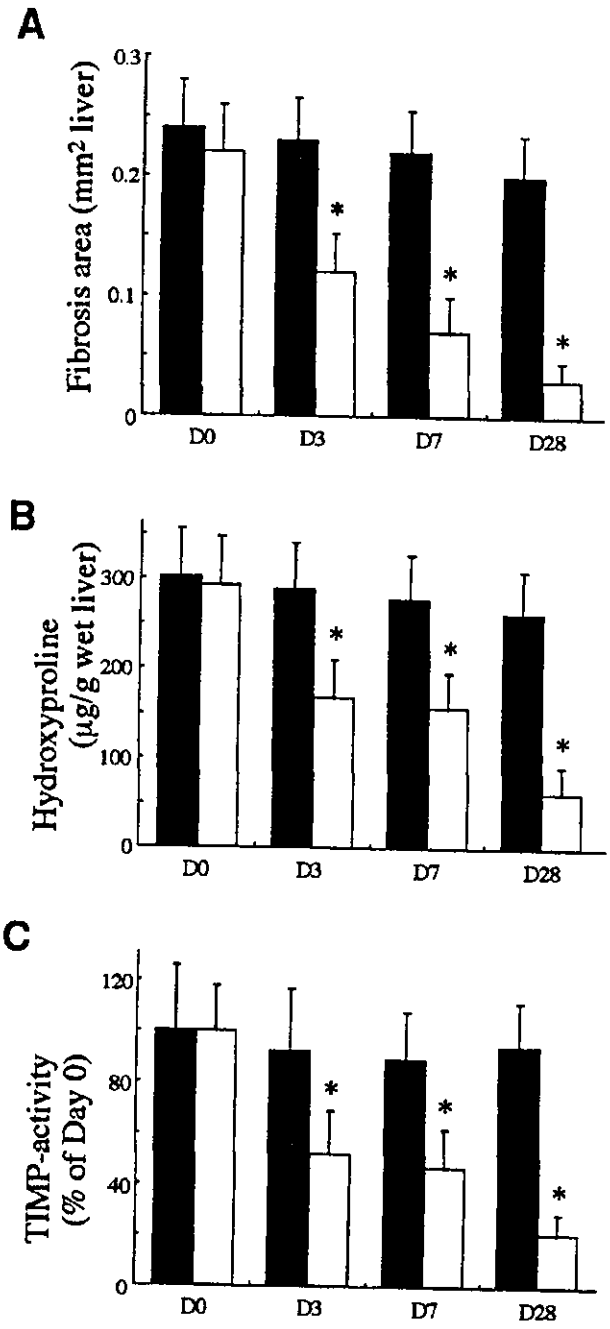

Fig. 2. Effect of TIMP-1 on (A) the fibrotic area, (B) hepatic hydroxyproline content, and (C) TIMP-1 biologic activity in the liver. Significant reductions of the fibrotic area and hydroxyproline content were found even by day 3 in the Cont mice (□) as compared with the TIMP-Tg mice (■). The degree of reduction of these factors mostly corresponded to that of the TIMP-1 activity. The data represent means ± SD. Each group consisted of 5 mice. *A statistically significant difference as compared with the TIMP-Tg mice ($P < .01$). Cont, control hybrid mice; TIMP, TIMP-Tg mice; D 0, 3, 7, and 28, at the respective day during the spontaneous recovery from the peak fibrosis (D 0: 3 days after the last injection of CCl_4).

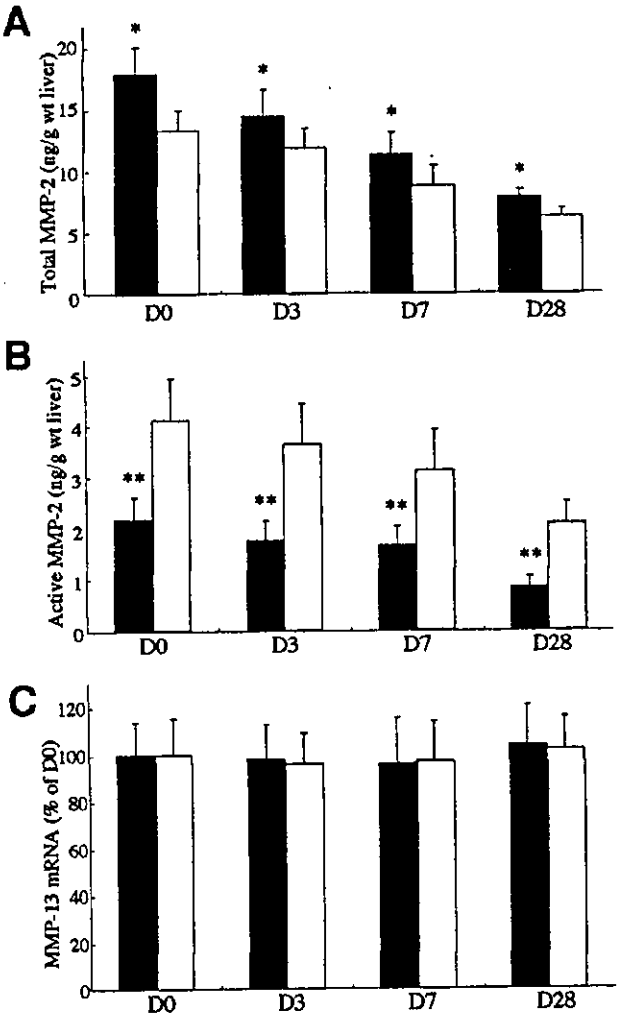

Fig. 3. The MMP-2 and MMP-13 expressions in the liver of the TIMP-Tg mice (■) and Cont mice (□). (A) The sum total (pro and active) MMP-2 levels were higher in the TIMP-Tg mice than in the Cont mice at the respective period. During the experiment, the MMP-2 level decreased by time in both the TIMP-Tg mice and Cont mice. (B) The active form of MMP-2 protein level in the liver of the TIMP-Tg mice was significantly lower than that of the Cont mice during the experiment ($P < .01$). The MMP-2 level was measured by ELISA. (C) The MMP-13 mRNA expression was not significantly altered in both the TIMP-Tg mice and Cont mice throughout the experiment. The data represent means ± SD. Each group consisted of 5 mice. *, **Statistically significant difference as compared with the Cont mice ($P < .05$ and $P < .01$, respectively). Cont, control hybrid mice; TIMP, TIMP-Tg mice; D 0, 3, 7, and 28, at the respective day during the spontaneous recovery point from the peak fibrosis (D 0: 3 days after the last injection of CCl_4).

puter-assisted semiquantitative analysis of the α-SMA positive cells showed results similar to those of the the immunohistochemical analysis (Fig. 5A). Because HSC have been shown to be the main source of collagen synthesis in the fibrotic liver, we next examined the procollagen-(I) mRNA expression in the liver. Similar to the results of α-SMA analysis, the procollagen-(I) mRNA expression significantly decreased with time in the Cont mice, whereas mRNA synthesis was maintained in the TIMP-Tg mice (Fig. 5B).

Effect of TIMP-1 on the Nonparenchyma Apoptotic Cells in the Liver. We next examined the effect of TIMP-1 on the nonparenchyma apoptotic cells in the liver. The apoptotic cells in the nonparenchyma significantly increased in the Cont mice concomitant with the resolution of fibrosis (representative features are shown by the arrows in Fig. 6A). On the other hand, no marked difference could be observed in the TIMP-Tg mice throughout the experiment (Fig. 6B). At this time, we do not have direct evidence that these apoptotic cells in the nonparenchyma were identical to the activated HSC because we failed to achieve good double immunostaining with α-SMA and TUNEL. We, however, found that these cells were not Kupffer cells (ED-1 negative), and the distribution pattern of TUNEL-positive cells in nonparenchyma tissue was very similar to that of α-SMA (data not shown).

***Effect of TIMP-1 on HSC Apoptosis* In Vitro.** To elucidate the direct interaction between TIMP-1 and HSC apoptosis, we examined the effect of TIMP-1 on HSC apoptosis with isolated HSC. As shown in Fig. 7A, incubation of the activated HSC in serum-free environment induced DNA ladder formation in gel electrophoresis. Treatment with 50 ng/mL of rTIMP-1 significantly attenuated the DNA laddering, and 500 ng/mL of rTIMP-1, which corresponded to the comparable circulation level in the TIMP-Tg-mouse,[20] almost completely inhibited the activated HSC apoptosis. We also examined the apoptotic index using the ELISA assay kit. Similar to DNA ladder formation, TIMP-1 treatment significantly attenuated the HSC apoptosis in a dose-dependent manner (Fig. 7B). It has been shown that caspase-3 plays an important role in apoptosis and that it is a central enzyme in the proapoptotic cascade.[33] We also examined the caspase-3 activity in response to TIMP-1 administration. Similar to a recent report,[25] we found that TIMP-1 significantly reduced the caspase-3 activity in the activated HSC in a dose-dependent manner (Fig. 7C). In addition to serum deprivation, treatment with 50 μmol/L of cyclohexamide induced apoptosis in the activated HSC, and we observed inhibitory effects of TIMP-1 on apoptosis and caspase-3 activity similar to those noticed in the serum deprivation experiment (data not shown).

Discussion

In the present study, using the liver-targeted TIMP-1-Tg-mouse, we showed that overexpression of TIMP-1

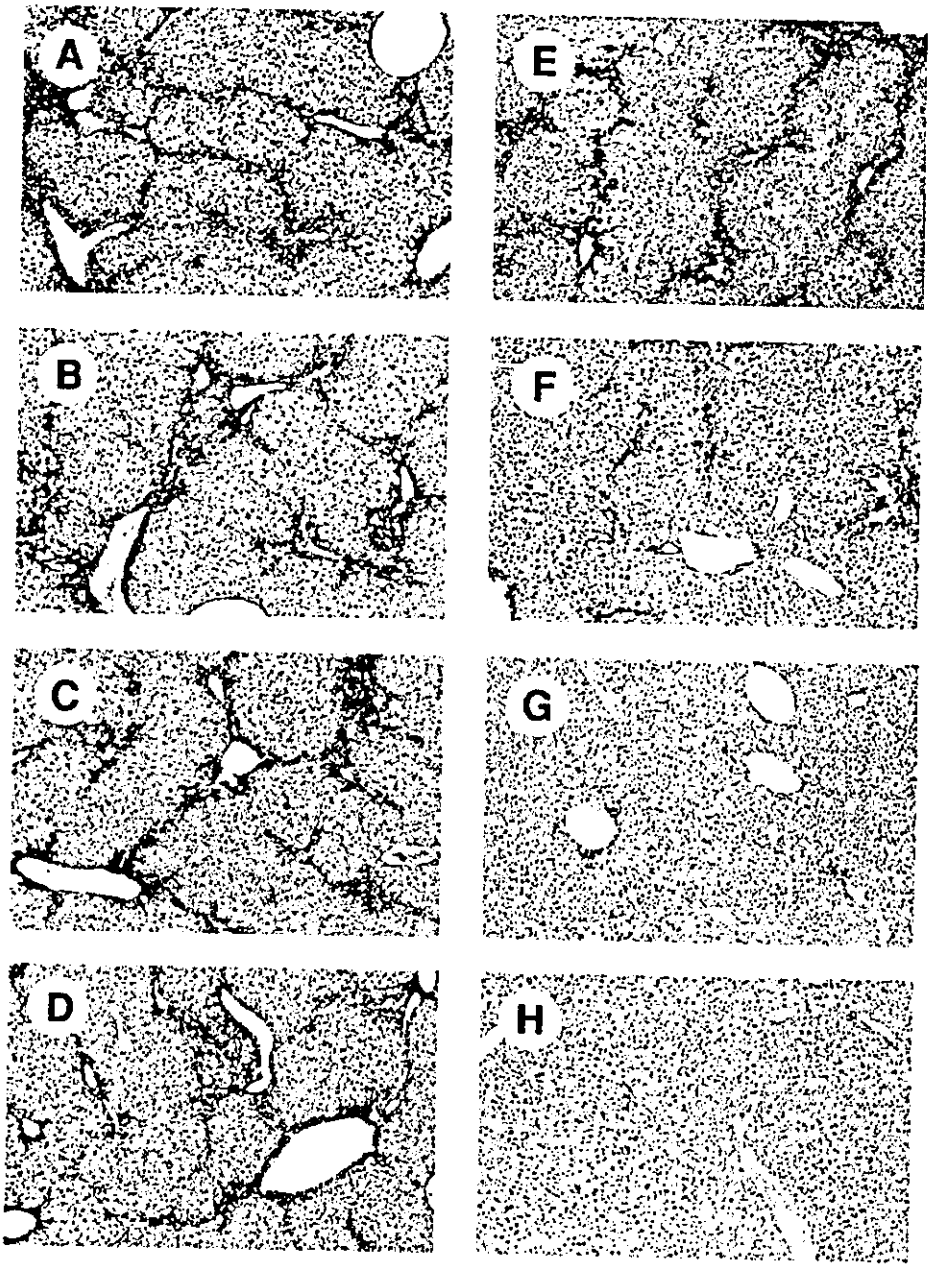

Fig. 4. Immunohistochemical analysis of α-SMA. The sections from the TIMP-Tg mice and Cont mice were taken on day 0 (TIMP: A, Cont: E), day 3 (TIMP: B, Cont: F), day 7 (TIMP: C, Cont: G), and day 28 (TIMP: D, Cont: H). Marked reductions of the α-SMA positive activated HSC were already apparently observed by day 3 in the Cont mice, whereas these immunopositivities were maintained in the TIMP-Tg mice during the experiment (original magnification ×40).

significantly suppressed spontaneous liver fibrosis resolution associated with down-regulation of the MMP activity and upkeep of the HSC activation. Furthermore, TIMP-1 markedly decreased the nonparenchyma apoptotic cells in the resolved liver and also inhibited HSC apoptosis *in vitro*.

It has been considered that, once established, fibrosis is irreversible for a long time. However, recent studies revealed that accumulation of ECM is not a static event but rather a dynamic state of disease in which there is a delicate balance between ECM production and degradation.[1-4] The ratio between MMP and TIMP expression has been shown to play an important role in ECM remodeling.[1-3] It has been reported that, during the course of fibrosis and cirrhosis, the TIMP-1 expression was significantly increased, whereas the interstitial collagenase (MMP-1) level remained relatively unchanged.[7-15] In the rat spontaneous liver fibrosis resolution model, the TIMP-1 expression returned rapidly to the control values with no marked changes in the rat interstitial collagenase (MMP-13).[7] We also found that the TIMP-1 activity decreased rapidly during spontaneous liver fibrosis reso-

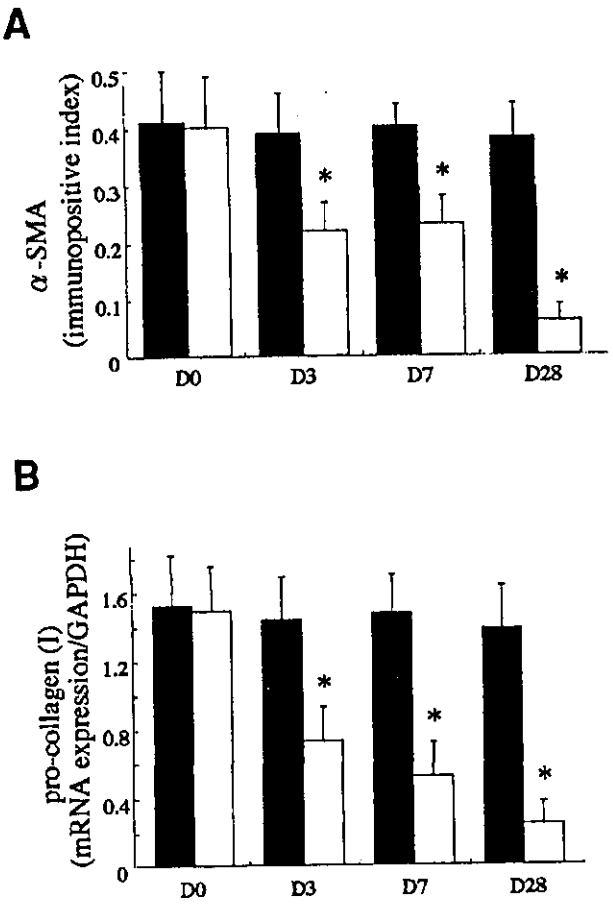

Fig. 5. Effect of TIMP-1 on HSC activation. (A) Computer-assisted semiquantitative analysis of the α-SMA positive cells in the liver. The α-SMA positive cells were significantly suppressed even by day 3 in the Cont mice (□) as compared with the TIMP-Tg mice (■). (B) The procollagen-(I) mRNA expression in the liver. The procollagen-(I) mRNA expression was measured by real-time PCR. Similar to the results of the α-SMA positive cells, the procollagen-(I) mRNA expression was significantly decreased with time in the Cont mice, whereas mRNA synthesis was sustained in TIMP-Tg mice. The suppression of procollagen-(I) mRNA was of similar magnitude to the inhibition of α-SMA positive cells. The data represent means ± SD. Each group consisted of 5 mice. *Statistically significant difference as compared with the TIMP-Tg mice ($P <$ .01). Cont, control hybrid mice; TIMP, TIMP-Tg mice; D 0, 3, 7, and 28, at the respective day during the spontaneous recovery point from the peak fibrosis (D 0: 3 days after the last injection of CCl_4).

lution in the Cont mice. This decrease in the MMP inhibitory activity allowed the active enzymes to resolve the established ECM. On the contrary, the biologic activity of TIMP-1 in the liver was sustained in the TIMP-Tg mice throughout the experiment by transgenic TIMP-1. The active form of MMP-2 was also significantly lower in the TIMP-Tg mice than in the Cont mice. There is no doubt that this net increase in the MMP inhibitory activity contributed to the attenuation of liver fibrosis resolution in the present study. It should be noted, however, that this alteration in the MMP and TIMP balance was not sufficient alone to explain this suppressive effect of TIMP-1. As we reported previously, TIMP-1 overexpression in the liver itself did not induce fibrosis development or ECM remodeling, suggesting that TIMP-1 did not affect HSC activation and initiation of fibrosis. It, however, significantly promoted fibrosis development upon fibrotic stimulation.[20] In other words, TIMP-1 showed a strong activity that promoted liver fibrosis development under the condition of HSC activation but not in the quiescent stage. Taken together, in addition to the MMP inhibitory activity, it is likely that the direct interaction between TIMP-1 and the activated HSC plays some role in ECM remodeling during the spontaneous resolution of liver fibrosis.

We found that the total MMP-2 level was higher in the TIMP-Tg mice than in the Cont mice, whereas the MMP-13 level was comparable in both groups during the resolution of liver fibrosis. We do not have an exact explanation for this different behavior of MMP family at this time. As described previously,[20] the MMP-2 level may reflect the feedback mechanism in response to the transgenic TIMP-1. It has been shown that MMP-2 and MMP-13 (MMP-1) exert different gene transcription mechanisms.[34,35] The MMP-2 promoter lesion lacks TATA box or TRE element, whereas MMP-1 possesses these elements like other MMPs. It would be possible that the different regulation mechanisms of the respective genes were involved in response to the constitutive high transgenic TIMP-1. Further studies are required to elucidate these interactions.

In addition to MMP inhibition, TIMP-1 is now recognized as a multifunctional protein. TIMP-1 has been reported to stimulate steroidogenesis, inhibit angiogenesis, and change the cell morphology; moreover, some of these biologic functions were independent of the MMP inhibitory effect.[6] Recently, it has been shown that TIMP-1 inhibits apoptosis in several types of cells, and this biologic effect is sometimes independent of MMP inhibition.[6,21-24] It has been recently shown that TIMP-1 exerted an antiapoptotic effect on the activated HSC in a dose-dependent manner and that this effect was mediated through MMP inhibition.[25] In the present study, we observed that the number of apoptotic cells in the nonparenchymal tissue was significantly higher in the Cont mice than in the TIMP-Tg mice, and the transposition pattern of the α-SMA positive cells and the procollagen-(I) mRNA expression almost corresponded with each other. We also found that TIMP-1 inhibited HSC apoptosis *in vitro*. Although we need to identify that these ongoing apoptotic cells in the nonparenchyma tissue were identi-

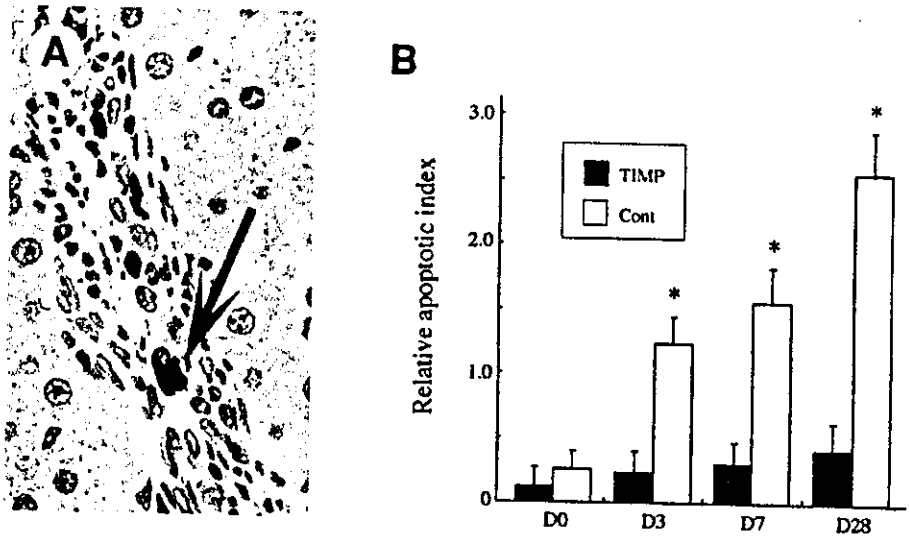

Fig. 6. Effect of TIMP-1 on the nonparenchyma apoptotic cells. (A) The **arrow** indicates the representative features of TUNEL positive apoptotic cells in the nonparenchyma. The distribution pattern of TUNEL positive cells was very similar to that of α-SMA positive cells. (B) Computer-assisted semiquantitative analysis of TUNEL-positive cells in the nonparenchyma. The apoptotic cells in the nonparenchyma were significantly increased in Cont mice even by day 3 as compared with the TIMP-Tg mice. The number of apoptotic cells was not significantly increased in the TIMP-Tg mice throughout the experiment. The data represent means ± SD. Each group consisted of 5 mice. *Statistically significant difference compared with the TIMP-Tg mice ($P < .01$). Cont, control hybrid mice; TIMP, TIMP-Tg mice; D 0, 3, 7, and 28, at the respective day during the spontaneous recovery from the peak fibrosis (D 0: 3 days after the last injection of CCl_4).

cal to the activated HSC, it is likely that these cells were, at least partly, activated HSC, and apoptosis of these activated HSC was inhibited by the transgenic TIMP-1, leading to less apparent spontaneous liver fibrosis resolution. On the other hand, in the Cont mice, the rapid decrease of TIMP-1 associated with HSC apoptosis caused an increase in the MMP activity and, consequently, promoted spontaneous liver fibrosis resolution.

Alternatively, it has been shown that TIMP-1 may act as a transcriptional factor.[36,37] It has been reported that

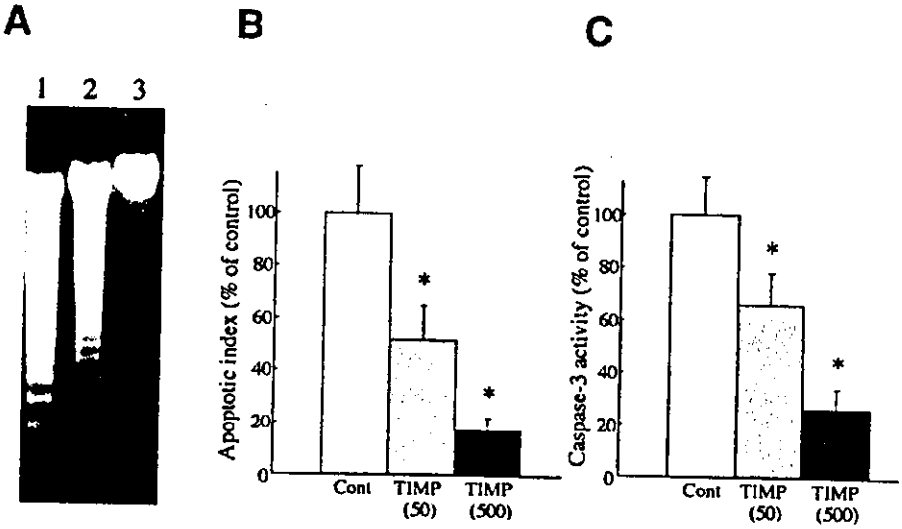

Fig. 7. Effect of TIMP-1 on activated HSC apoptosis and caspase-3 activity *in vitro*. Apoptosis was detected by (A) the DNA ladder formation in gel electrophoresis and by (B) ELISA assay kit. (C) The caspase-3 activity in the HSC in response to TIMP-1 was measured by the assay kit as described in the Materials and Methods section. The treatments with human recombinant TIMP-1 significantly suppressed the HSC apoptosis and caspase-3 activity in a dose-dependent manner. **Lane 1**: no-treatment control group; **lanes 2 and 3**: TIMP-1-treated groups at doses of 50 and 500 ng/mL, respectively. The data in (B) and (C) represent means ± SD (n = 5). *Statistically significant difference as compared with the control group ($P < .01$).

TIMP-1 can translocate into the nucleus but that the other TIMP family factors such as TIMP-2 can not.[36] We previously showed that overexpression of TIMP-1 in the mammary carcinoma cells induced collagen-IV and laminin transcription.[38] It is possible that a high level of the transgenic TIMP-1 may somehow change the phenotype of HSC, thereby maintaining the activation of HSC.

In summary, we have shown that TIMP-1 overexpression in the liver significantly attenuated spontaneous liver fibrosis resolution. This effect was possibly achieved with the combination of a net decrease of the MMP inhibitory activity and the suppression of HSC apoptosis by TIMP-1.

References

1. Olaso E, Friedman SL. Molecular regulation of hepatic fibrogenesis. J Hepatol 1998;29:836-847.
2. Arthur MJ. Degradation of matrix proteins in liver fibrosis. Pathol Res Pract 1994;190:825-833.
3. Woessner JF Jr. Matrix metalloproteinases and their inhibitors in connective tissue remodeling. FASEB J 1991;5:2145-2154.
4. Bonis PA, Friedman SL, Kaplan MM. Is liver fibrosis reversible? N Engl J Med 2001;344:452-454.
5. Dufour JF, DeLellis R, Kaplan MM. Regression of hepatic fibrosis in hepatitis C with long-term interferon treatment. Dig Dis Sci 1998;43: 2573-2576.
6. Gomez DE, Alonso DF, Yoshiji H, Thorgeirsson UP. Tissue inhibitors of metalloproteinases: structure, regulation and biological functions. Eur J Cell Biol 1997;74:111-122.
7. Iredale JP, Benyon RC, Pickering J, McCullen M, Northrop M, Pawley S, Hovell C, et al. Mechanisms of spontaneous resolution of rat liver fibrosis. Hepatic stellate cell apoptosis and reduced hepatic expression of metalloproteinase inhibitors. J Clin Invest 1998;102:538-549.
8. Iredale JP, Benyon RC, Arthur MJ, Ferris WF, Alcolado R, Winwood PJ, Clark N, et al. Tissue inhibitor of metalloproteinase-1 messenger RNA expression is enhanced relative to interstitial collagenase messenger RNA in experimental liver injury and fibrosis. HEPATOLOGY 1996;24:176-184.
9. Kossakowska AE, Edwards DR, Lee SS, Urbanski LS, Stabbler AL, Zhang CL, Phillips BW, et al. Altered balance between matrix metalloproteinases and their inhibitors in experimental biliary fibrosis. Am J Pathol 1998;153: 1895-1902.
10. Herbst H, Wege T, Milani S, Pellegrini G, Orzechowski HD, Bechstein WO, Neuhaus P, et al. Tissue inhibitor of metalloproteinase-1 and -2 RNA expression in rat and human liver fibrosis. Am J Pathol 1997;150: 1647-1659.
11. Murawaki Y, Yamamoto H, Kawasaki H, Shima H. Serum tissue inhibitor of metalloproteinases in patients with chronic liver disease and with hepatocellular carcinoma. Clin Chim Acta 1993;218:47-58.
12. Watanabe T, Niioka M, Hozawa S, Kameyama K, Hayashi T, Arai M, Ishikawa A, et al. Gene expression of interstitial collagenase in both progressive and recovery phase of rat liver fibrosis induced by carbon tetrachloride. J Hepatol 2000;33:224-235.
13. Arthur MJ, Mann DA, Iredale JP. Tissue inhibitors of metalloproteinases, hepatic stellate cells and liver fibrosis. J Gastroenterol Hepatol 1998; 13(Suppl):S33-S38.
14. Iredale JP. Tissue inhibitors of metalloproteinases in liver fibrosis. Int J Biochem Cell Biol 1997;29:43-54.
15. Nakatsukasa H, Ashida K, Higashi T, Ohguchi S, Tsuboi S, Hino N, Nouso K, et al. Cellular distribution of transcripts for tissue inhibitor of metalloproteinases 1 and 2 in human hepatocellular carcinomas. HEPATOLOGY 1996;24:82-88.
16. Benyon RC, Iredale JP, Goddard S, Winwood PJ, Arthur MJ. Expression of tissue inhibitor of metalloproteinases 1 and 2 is increased in fibrotic human liver. Gastroenterology 1996;110:821-831.
17. Murawaki Y, Ikuta Y, Idobe Y, Kitamura Y, Kawasaki H. Tissue inhibitor of metalloproteinase-1 in the liver of patients with chronic liver disease. J Hepatol 1997;26:1213-1219.
18. Kasahara A, Hayashi N, Mochizuki K, Oshita M, Katayama K, Kato M, Masuzawa M, et al. Circulating matrix metalloproteinase-2 and tissue inhibitor of metalloproteinase-1 as serum markers of fibrosis in patients with chronic hepatitis C. Relationship to interferon response. J Hepatol 1997; 26:574-583.
19. Milani S, Herbst H, Schuppan D, Grappone C, Pellegrini G, Pinzani M, Casini A, et al. Differential expression of matrix-metalloproteinase-1 and -2 genes in normal and fibrotic human liver. Am J Pathol 1994;144:528-537.
20. Yoshiji H, Kuriyama S, Miyamoto Y, Thorgeirsson UP, Gomez DE, Kawata M, Yoshii J, et al. Tissue inhibitor of metalloproteinases-1 promotes liver fibrosis development in a transgenic mouse model. HEPATOLOGY 2000;32:1248-1254.
21. Guedez L, Courtemanch L, Stetler-Stevenson M. Tissue inhibitor of metalloproteinase (TIMP)-1 induces differentiation and an antiapoptotic phenotype in germinal center B cells. Blood 1998;92:1342-1349.
22. Li G, Fridman R, Kim HR. Tissue inhibitor of metalloproteinase-1 inhibits apoptosis of human breast epithelial cells. Cancer Res 1999;59:6267-6275.
23. Guedez L, Stetler-Stevenson WG, Wolff L, Wang J, Fukushima P, Mansoor A, Stetler-Stevenson M. *In vitro* suppression of programmed cell death of B cells by tissue inhibitor of metalloproteinases-1. J Clin Invest 1998; 102:2002-2010.
24. Guedez L, McMarlin AJ, Kingma DW, Bennett TA, Stetler-Stevenson M, Stetler-Stevenson WG. Tissue inhibitor of metalloproteinase-1 alters the tumorigenicity of Burkitt's lymphoma via divergent effects on tumor growth and angiogenesis. Am J Pathol 2001;158:1207-1215.
25. Murphy FR, Issa R, Zhou X, Ratnarajah S, Nagase H, Arthur MJ, Benyon C, et al. Inhibition of apoptosis of activated hepatic stellate cells by tissue inhibitor of metalloproteinase-1 is mediated via effects on matrix metalloproteinase inhibition. Implications for reversibility of liver fibrosis. J Biol Chem 2002; 277:11069-11076.
26. Yoshiji H, Kuriyama S, Ways DK, Yoshii J, Miyamoto Y, Kawata M, Ikenaka Y, et al. Protein kinase C lies on the signaling pathway for vascular endothelial growth factor-mediated tumor development and angiogenesis. Cancer Res 1999;59:4413-4418.
27. Yoshiji H, Kuriyama S, Yoshii J, Ikenaka Y, Noguchi R, Nakatani T, Tsujinoue H, et al. Angiotensin-II type 1 receptor interaction is a major regulator for liver fibrosis development in rats. HEPATOLOGY 2001;34:745-750.
28. Gautschi O, Tschopp S, Olie RA, Leech SH, Simoes-Wust AP, Ziegler A, Baumann B, et al. Activity of a novel bcl-2/bcl-xL-bispecific antisense oligonucleotide against tumors of diverse histologic origins. J Natl Cancer Inst 2001;93:463-471.
29. Yasuda M, Shimizu I, Shiba M, Ito S. Suppressive effects of estradiol on dimethylnitrosamine-induced fibrosis of the liver in rats. HEPATOLOGY 1999;29:719-727.
30. Watanabe T, Niioka M, Ishikawa A, Hozawa S, Arai M, Maruyama K, Okada A, et al. Dynamic change of cells expressing MMP-2 mRNA and MT1-MMP mRNA in the recovery from liver fibrosis in the rat. J Hepatol 2001;35:465-473.
31. Lee HS, Huang GT, Miau LH, Chiou LL, Chen CH, Sheu JC. Expression of matrix metalloproteinases in spontaneous regression of liver fibrosis. Hepatogastroenterology 2001;48:1114-1117.
32. Takahara T, Furui K, Funaki J, Nakayama Y, Itoh H, Miyabayashi C, Sato H, et al. Increased expression of matrix metalloproteinase-II in experimental liver fibrosis in rats. HEPATOLOGY 1995;21:787-795.

33. Frisch SM, Morisaki JH. Positive and negative transcriptional elements of the human type IV collagenase gene. Mol Cell Biol 1990;10:6524-6532.
34. Porter AG, Janicke RU. Emerging roles of caspase-3 in apoptosis. Cell Death Differ 1999;6:99-104.
35. Sato H, Seiki M. Regulatory mechanism of 92 kDa type IV collagenase gene expression which is associated with invasiveness of tumor cells. Oncogene 1993;8:395-405.
36. Zhao WQ, Li H, Yamashita K, Guo XK, Hoshino T, Yoshida S, Shinya T, et al. Cell cycle-associated accumulation of tissue inhibitor of metalloproteinases-1 (TIMP-1) in the nuclei of human gingival fibroblasts. J Cell Sci 1998;111:1147-1153.
37. Ritter LM, Garfield SH, Thorgeirsson UP. Tissue inhibitor of metalloproteinases-1 (TIMP-1) binds to the cell surface and translocates to the nucleus of human MCF-7 breast carcinoma cells. Biochem Biophys Res Commun 1999;257:494-499.
38. Yoshiji H, Harris SR, Raso E, Gomez DE, Lindsay CK, Shibuya M, Sinha CC, et al. Mammary carcinoma cells over-expressing tissue inhibitor of metalloproteinases-1 show enhanced vascular endothelial growth factor expression. Int J Cancer 1998;75:81-87.

Cyclins and Cyclin-Dependent Kinases: Comparative Study of Hepatocellular Carcinoma Versus Cirrhosis

Tsutomu Masaki,[1] Yasushi Shiratori,[2] William Rengifo,[2] Kouichi Igarashi,[2] Michiko Yamagata,[2] Kazutaka Kurokohchi,[1] Naohito Uchida,[1] Yoshiaki Miyauchi,[1] Hitoshi Yoshiji,[3] Seishiro Watanabe,[1] Masao Omata,[2] and Shigeki Kuriyama[1]

Increasing evidence has indicated that perturbation of cyclins is one of the major factors leading to cancer. The aim of this study was not only to investigate various cell cycle-related kinase activities in hepatocellular carcinoma (HCC), but also to analyze the difference of cell cycle-related kinase activity levels between hepatitis C virus (HCV)-induced HCC and HCV-induced cirrhosis. The protein levels of cyclins D1, E, A, and H, and of cyclin dependent kinase 1 (Cdk1), Cdk2, Cdk4, Cdk6, and Cdk7 in HCC and in surrounding nontumorous cirrhosis were determined by Western blot. The enzymatic activities of cyclins D1, E, A, Cdk1, Cdk4, Cdk6, Cdk7, and Wee1 were measured using *in vitro* kinase assays. Protein levels and kinase activities of cyclin D1, Cdk4, cyclin E, cyclin A, and Wee1 were significantly elevated in HCC compared with surrounding cirrhotic tissues. The enhanced cyclin D1-related kinase activity in HCC was accompanied by the up-regulation of Cdk4 activity, but not Cdk6 activity. The kinase activities of Cdk6, Cdk7, and Cdk1 did not differ between HCC and surrounding cirrhotic tissues. In addition, the protein levels and kinase activities of cyclin D1, Cdk4, and cyclin E were higher in poorly differentiated HCC and advanced HCC. In conclusion, the increases of cyclin D1, Cdk4, cyclin E, cyclin A, and Wee1 play an important role in the development of HCC from cirrhosis. Cyclin D1, Cdk4, and cyclin E activation may be closely related to the histopathologic grade and progression of HCC. (HEPATOLOGY 2003;37:534-543.)

Recent studies, including our research, have revealed that the deranged expression of cell cycle-related proteins is one of the major factors contributing to hepatocellular carcinoma (HCC) development.[1-6] Here we investigated biochemical differences of various cell cycle-related kinase activities and protein levels in cirrhosis and HCC.

Specific cyclin/cyclin-dependent kinase (Cdk) complexes are activated at different intervals during the cell cycle.[7-15] Cyclin D1/Cdk4 and cyclin D1/Cdk6 are activated in mid-G1 (Fig. 1, phase 1), whereas cyclin E/Cdk2 complexes are required for the G1/S transition (Fig. 1, phase 2), cyclin A/Cdk2 for the progression of DNA synthesis (Fig. 1, phase 3), and cyclin A-B/Cdk1 for the G2/M transition (Fig. 1, phase 4) of mitosis. The activation of cyclin D1/Cdk4 and cyclin D1/Cdk6 complexes at mid-G1 is responsible for the phosphorylation of retinoblastoma protein (pRb), and 2 Rb related proteins, p107, and p130. Members of the pRb family form complexes with transcription factors of the E2F family.[16] This interaction with pRb family members blocks the transcriptional activity of E2Fs; the complexes formed also function as active transcriptional repressor complexes at the promoters of some cell cycle genes. Phosphorylation of the pRb family inhibits the interaction with E2F family transcription factor and permits the expression of genes necessary for S-phase entry (cyclin A, proliferating cell nuclear antigen, and so on).[17] The expression of cyclins E and A at mid- to late-G1 permits the formation of cyclin E/Cdk2 and cyclin A/Cdk2 complexes, which need to be activated by the Cdk activating kinase, Cdk7[12] (Fig. 1, phase 5). Cyclin H is regulated by Cdk7, and the complex of cyclin H and Cdk7 phosphorylates Cdk1, Cdk2, Cdk4, and Cdk6 at specific regulatory threonine sites,

Abbreviations: HCC, hepatocellular carcinoma; Cdk, cyclin-dependent kinase; pRb, retinoblastoma protein; HCV, hepatitis C virus; HBV, hepatitis B virus; IgG, immunoglobulin G.

From the [1]Third Department of Internal Medicine, Kagawa Medical University, Kagawa, Japan; the [2]Department of Gastroenterology, Faculty of Medicine, University of Tokyo, Tokyo, Japan; and the [3]Third Department of Internal Medicine, Nara Medical University, Nara, Japan.

Received March 5, 2002; accepted December 20, 2002.

Supported by a Grant for Scientific Research from the Ministry of Education, Science, and Culture of Japan.

Address reprint requests to: Tsutomu Masaki, M.D., PhD., Third Department of Internal Medicine, Kagawa Medical University, 1750-1 Ikenobe, Miki-cho, Kagawa 761-0793, Japan. E-mail: tmasaki@kms.ac.jp; fax: (81) 87-891-2158.

0270-9139/03/3703-0009$30.00/0

doi:10.1053/jhep.2003.50112

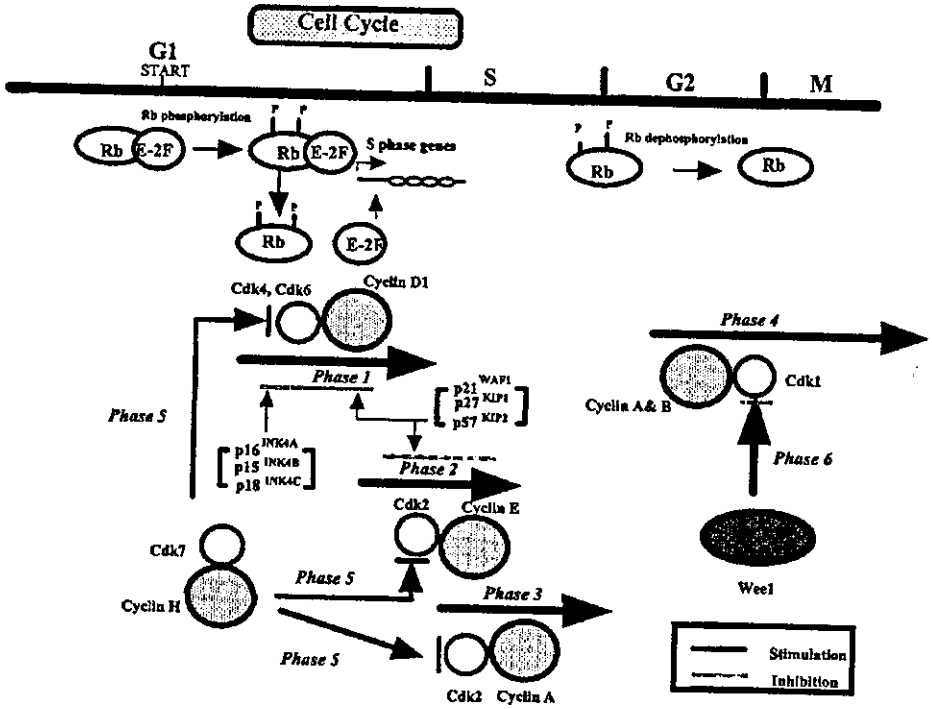

Fig. 1. Cell cycle regulators studied in the present research. A highly schematic view of points of action of mammalian cyclin-Cdk complexes in the cell cycle is shown here. Enzymes controlling the cell cycle include Cdks, which are activated by binding to cyclins. Complexes of Cdk4 and Cdk6 with cyclin D1 are required for G1 phase progression (phase 1). Further progression through G1 requires cyclin E (phase 2), and passage through S phase requires cyclin A (phase 3), each in a complex with Cdk2. The complex of cyclin B/Cdk1 is required for the G2 to M phase transition (phase 4). Cyclin H is one such regulatory subunit that preferentially binds to Cdk7 and forms a cyclin H/Cdk7 complex, which can then phosphorylate Cdk1, Cdk2, and Cdk4 to regulate cell cycle progression (phase 5). Wee1 has been identified as a protein kinase that suppresses entry into mitosis by inhibiting tyrosine phosphorylation of cell division cycle (Cdk1) (phase 6). Cdk activity is curtailed by various inhibitors, including $p16^{INK4A}$, $p15^{INK4B}$, $p18^{INK4C}$, $p21^{WAF1}$, $p27^{KIP1}$ and $p57^{KIP2}$. Hypophosphorylated pRb forms complexes with E2F family trancription factors, thus halting the cell cycle. G1 cyclins (D and E cyclins), in complex with Cdks, phosphorylate pRb (pRb), releasing bound transcription factors such as E2F, which activate genes required for S-phase entry. In the figure, only the cyclins are shaded, to aid in distinguishing them from Cdks and other proteins.

leading to the up-regulation of kinase activities.[12] Wee1 has been identified as a tyrosine protein kinase that phosphorylates Cdk1 at tyrosine 15,[13] and the effect of Wee1 activation is to maintain Cdk1 in an inactivated state (Fig. 1, phase 6).

Although there is increasing evidence that perturbation of cell cycle regulation is one of the important factors contributing to cancer, there have been few studies showing the relationship between cyclins and human HCC.[1-6] Previous reports described changes of only 2 cyclins (cyclin A and cyclin D1) in HCC, but they did not show a clear relationship between general derangement of other cyclins or cyclin-related kinase activities and HCC.

We previously reported that overexpression of cyclins D1, E, and A and of Cdk4 was detected in preneoplastic and neoplastic liver of Long Evans Cinnamon rats,[18] an HCC animal model rat.[19] In addition, Pascale et al.[20] also showed that overexpresssion of cyclins D1, E, and A messenger RNA and protein and the overexpression of cyclin D1/Cdk4 and cyclin E/Cdk2 complexes occurred in HCC of chemically induced HCC of Fischer 344 rats. These previous data suggest the possibility that cell cycle–related proteins, including cyclins and Cdks other than cyclins A, D1, and E, might play a role in the carcinogenesis or progression of human HCC. In fact, overexpression of cyclin B1, Cdk1, Cdk2, and Cdk4 also has been shown in human cancers other than HCC.[21-24] Based on these facts, it is of interest to examine other cell cycle–related proteins, including various cyclins and Cdks, as related to the carcinogenesis or progression in human HCC.

In this study, we analyzed cell cycle-related kinase activities, namely, the activities of cyclin D1, Cdk4, Cdk6, cyclin E, cyclin A, Cdk1, Cdk7, and Wee1, not only in hepatitis C virus (HCV)–induced HCC, but also in surrounding nontumorous cirrhosis, and examined what kinds of cyclin or Cdk are important for the development of HCC from cirrhosis. In addition, we also investigated the relationship between cell cycle–related kinase activities and the clinicohistopathologic characteristics of

Table 1. Patient Characteristics

Patient No.	Gender	Age	Virus	*Background Liver	Size of Tumor (cm)	†TNM	‡Histology
1	M	67	C	F4	2.0	I	WD
2	M	57	C	F4	1.8	I	WD
3	F	58	C	F4	1.6	I	WD
4	M	72	C	F4	1.8	I	WD
5	M	61	C	F4	6.2	II	MD
6	M	67	C	F4	2.5	II	MD
7	M	67	C	F4	7.8	II	MD
8	F	63	C	F4	12.0	II	MD
9	F	65	C	F4	2.5	II	MD
10	M	65	C	F4	6.5	II	MD
11	M	59	C	F4	3.2	II	MD
12	F	72	C	F4	7.5	IVb	PD
13	M	59	C	F4	3.0	II	PD
14	F	75	C	F4	8.0	IVa	PD
15	M	54	C	F4	4.5	II	PD
16	M	58	C	F4	7.9	IVa	PD
17	M	65	C	F4	8.5	III	PD
18	M	60	C	F4	7.5	III	PD
19	M	69	C	F4	12.5	IVa	PD
20	M	60	C	F4	5.2	IVa	PD
21	M	56	–	F0			
22	F	58	–	F0			
23	M	60	–	F0			
24	M	60	–	F0			
25	M1	67	–	F0			

Abbreviations: M, male; F, female; C, hepatitis C virus; –, negative; WD, well differentiated; MD, moderately differentiated; PD, poorly differentiated.

*The fibrotic stage in surrounding tissues was assessed using Desmet's classification.

†TNM was classified as proposed by the International Union Against Cancer and American Joint Committee on Cancer.

‡Histological grading of HCC was classified using the criteria of the International Working Party.

HCC. The present study is the first report on a series of cyclin-related kinase activities in human HCC.

Materials and Methods

Tissue Samples. Tissue samples, including the tumorous and the surrounding nontumorous cirrhotic tissues, were obtained from 20 patients with HCC during surgery (15 men and 5 women; mean age, 63.7 ± 5.7 years; range, 54 to 75 years) (Table 1, patients 1 through 20). All the patients were HCV-RNA–positive, as determined by the reverse-transcriptase polymerase chain reaction method.[25] The clinicopathologic data for these patients are also shown in Table 1. Five normal liver tissue samples also were obtained from patients with liver metastases of colon cancer (4 men and 1 woman; mean age, 60.2 ± 4.2 years; range, 56 to 67 years) during surgery (Table 1, patients 21 through 25). All the serum samples from these patients were negative for hepatitis B virus (HBV) and HCV. The histologic grade of HCC, the fibrotic stage of the surrounding tissues, and the classification of primary tumor regional lymph nodes, distant metastasis (pTNM) were determined according to the criteria of the International Working party,[26] Desmet's classification,[27] and the criteria of the International Union Against Cancer and the American Joint Committee on Cancer,[28] respectively.

Chemicals and Antibodies. Chemicals were obtained from Sigma Chemical Co. (Tokyo, Japan) or Wako Pure Chemical Co. (Tokyo, Japan). All primary antibodies were purchased from Santa Cruz Biotechnology (Tokyo, Japan), except for anti-Cdk2 polyclonal antibody, which was purchased from Transduction Laboratories (Tokyo, Japan) and antiphosphoserine Rb antibody, which was obtained from MBL Co. Ltd (Nagoya, Japan). All secondary antibodies were purchased from Amersham Life Science (Tokyo, Japan). Optimal dilutions of antibodies used for Western blot in this study were as follows: monoclonal antibody HD11 (anti-cyclin D1), 1:100; polyclonal antibody H303 (anti-Cdk4), 1:100; polyclonal antibody C-21(anti-Cdk6), 1:100; polyclonal antibody M-20 (anti-cyclin E), 1:100; monoclonal antibody 55 (anti-Cdk2), 1:250; monoclonal antibody BF683 (anti-cyclin A), 1:100; polyclonal antibody N-19 (anti-Cdk7), 1:100; polyclonal antibody c-20 (anti-Wee1), monoclonal antibody C-15 (anti-Rb), 1:400; polyclonal antibody Ser 780 (anti-phosphoserine Rb), 1:1,000; monoclonal antibody TU-02 (α-tubulin), 1:100; horseradish peroxidase anti–mouse immunoglobulin G (IgG), 1:1,000; horseradish peroxidase–anti-rabbit IgG, 1:1,000. Antibody C-15 against pRb recognizes both phosphorylated and nonphosphorylated Rb. The phosphoserine Rb polyclonal antibody (Ser 780) reacts only with phosphorylated pRb at Ser 780, and detects a 105 kDa protein corresponding to human pRb that includes amino acids 774-786. Cyclin D1/Cdk4 specifically phosphorylates Ser 780 in pRb.[29]

Tissue Lysates. The tissue samples were frozen on dry ice within 20 minutes after collection. The tissue lysate was prepared as described by our previous report.[18] Protein concentration was measured using a dye-binding protein assay based on the Bradford method.[30]

Gel Electrophoresis and Western Blot. Sodium dodecyl sulfate-polyacrylamide gel electrophoresis was performed according to the method of Laemmli,[31] and Western blot was performed as described by Towbin et al.[32] Immunoreactive proteins were visualized with an enhanced chemiluminescence detection system (Amersham, Tokyo, Japan) and radiographic film.

Kinase Activities of Various Cyclins and Cdks. The kinase activities of various cyclins and Cdks were performed by autoradiography, as described by our previous report.[18] Phosphorylated pRb, histone H1, and Cdk1

bands obtained from autoradiography were visualized by image analysis using a BAS 2000 system (Fuji Film, Tokyo, Japan).

Densitometric Analysis. The densities of the phosphorylated bands of Rb fusion protein, histone H1, and Cdk1 obtained by autoradiography were quantitated by means of densitometric scanning (Tlc scanner; Shimazu, Co. Ltd, Kyoto, Japan). The kinase activity in HCC and adjacent nontumorous cirrhotic tissues was expressed relative to that in the normal liver. The densities of the immunoreactive bands of the various cyclin-related proteins obtained by Western blot analysis also were analyzed and calculated as the ratio relative to that in the normal liver.

Statistical Analysis. The significance of differences in Figs. 2K, 3I, and 5 was analyzed by Scheffe's test.[33] The significance of differences in Figs. 4C, 4D, and 6D was analyzed by the Mann-Whitney *U* test. These data were expressed as mean ± SEM. The relationship among cyclin D1, Cdk4, and Cdk6 activities was studied using Pearson's coefficient test.

Results

Western Blot of Cell Cycle–Related Proteins. Patient numbers in Fig. 2A through 2J correspond to those in Table 1. The cyclin D1, Cdk4, cyclin E, and cyclin A in moderately and/or poorly differentiated HCC were higher than those in surrounding cirrhotic tissues (Fig. 2A, B, D, and F). In contrast, the levels of Cdk6, Cdk2, Cdk1, cyclin H, and Cdk7 did not differ between nontumorous cirrhotic and tumorous tissue (Fig. 2C, E, G, H, and I). The levels of cyclin D1, Cdk4, Cdk6 cyclin E, cyclin A, and Cdk1 in normal liver were very low (Fig. 2A through D and F through G). The expression of Wee1 could not be detected in any liver samples, including HCC samples, by Western blot analysis. The amount of α-tubulin (an internal control for protein loading) was almost the same in each lane in sodium dodecyl sulfate polyacrylamide gel electrophoresis (Fig. 2J). The mean levels of cyclin D1, Cdk4, cyclin E, and cyclin A proteins in tumorous tissues were significantly elevated compared with surrounding cirrhotic tissues (Fig. 2K).

Activity of Cell Cycle–Related Kinases. Although cyclin D1 (Fig. 3A), Cdk4 (Fig. 3B), cyclin E (Fig. 3D), and cyclin A (Fig. 3E) activities were detected not only in HCC, but also in nontumorous cirrhosis, they were markedly higher in poorly differentiated HCC. In contrast, the level of Cdk6, Cdk1, and Cdk7 activities was about the same in nontumorous cirrhotic and tumorous tissues (Fig. 3C, F, and G). The enhancement cyclin D1–related kinase activity in HCC was strongly correlated with the up-regulation of Cdk4 activity ($r = 0.94$, $P < .001$), but not Cdk6 activity. The levels of cyclin D1, Cdk4, Cdk6, cyclin E, cyclin A, Cdk1, and Wee1 activities in normal liver were very low (Fig. 3A through F, H), whereas the level of Cdk7 activity was found to be about the same in normal liver, HCC, and surrounding nontumorous cirrhotic tissues (Fig. 3G). Wee1 kinase activity was found to be increased in most HCCs, irrespective of tumor differentiation. No phosphorylated pRb or histone H1 was detected in kinase assays with the immunoprecipitation product from liver tissues obtained with nonimmune mouse IgG or nonimmue rabbit IgG as the negative control (data not shown). The mean levels of cyclin D1, Cdk4, Cdk6, cyclin E, cyclin A, and Wee1 kinases were significantly elevated compared with surrounding cirrhotic tissues (Fig. 3I).

pRb Phosphorylation. The level of pRb did not undergo significant variation among the HCC samples tested in this study, but it was much more highly phosphorylated in HCC, as suggested by the fact that the pRb band was sifted in tumorous tissues as compared with nontumorous cirrhotic tissues and normal liver (Fig. 4A). We also analyzed whether one of the pRb phosphorylation sites, Ser 780, was phosphorylated or not. In Western blot analysis with antibody specific for pRb phosphorylated at Ser 780, the intensity of the phosphorylated pRb band in HCC was stronger than that in nontumorous cirrhotic tissues (Fig. 4B). A band corresponding to the pRb phosphorylated at Ser 780 was detected in HCCs of cases 7 through 14, 16, and 18 through 20, but was not detected in the other cases described in Table 1. Phosphorylated pRb was not detected in any normal liver samples.

In addition, we studied the levels of the cell cycle–related kinase activities and the corresponding proteins in HCC with and without phosphorylated pRb. The mean levels of kinase activities of cyclin D1, Cdk4, cyclin E, and cyclin A in HCC with pRb phosphorylation were significantly higher than those in HCC without pRb phosphorylation (Fig. 4C). On the other hand, the mean levels of cyclin E protein in HCC with pRb phosphorylation was significantly higher than those in HCC without pRb phosphorylation (Fig. 4D).

Relationship Between Various Cell Cycle–Related Kinase Activities and the Characteristics of HCC. Analysis of the various cell cycle–related kinase activities in relation to the grade of HCC differentiation revealed that the kinase activities of cyclin D1, Cdk4, and cyclin E were markedly increased in poorly differentiated HCC in comparison with those in well- and moderately differentiated HCC (Fig. 5A). Up-regulation of Wee1 kinase activity was detected in most cases of HCC, irrespective of

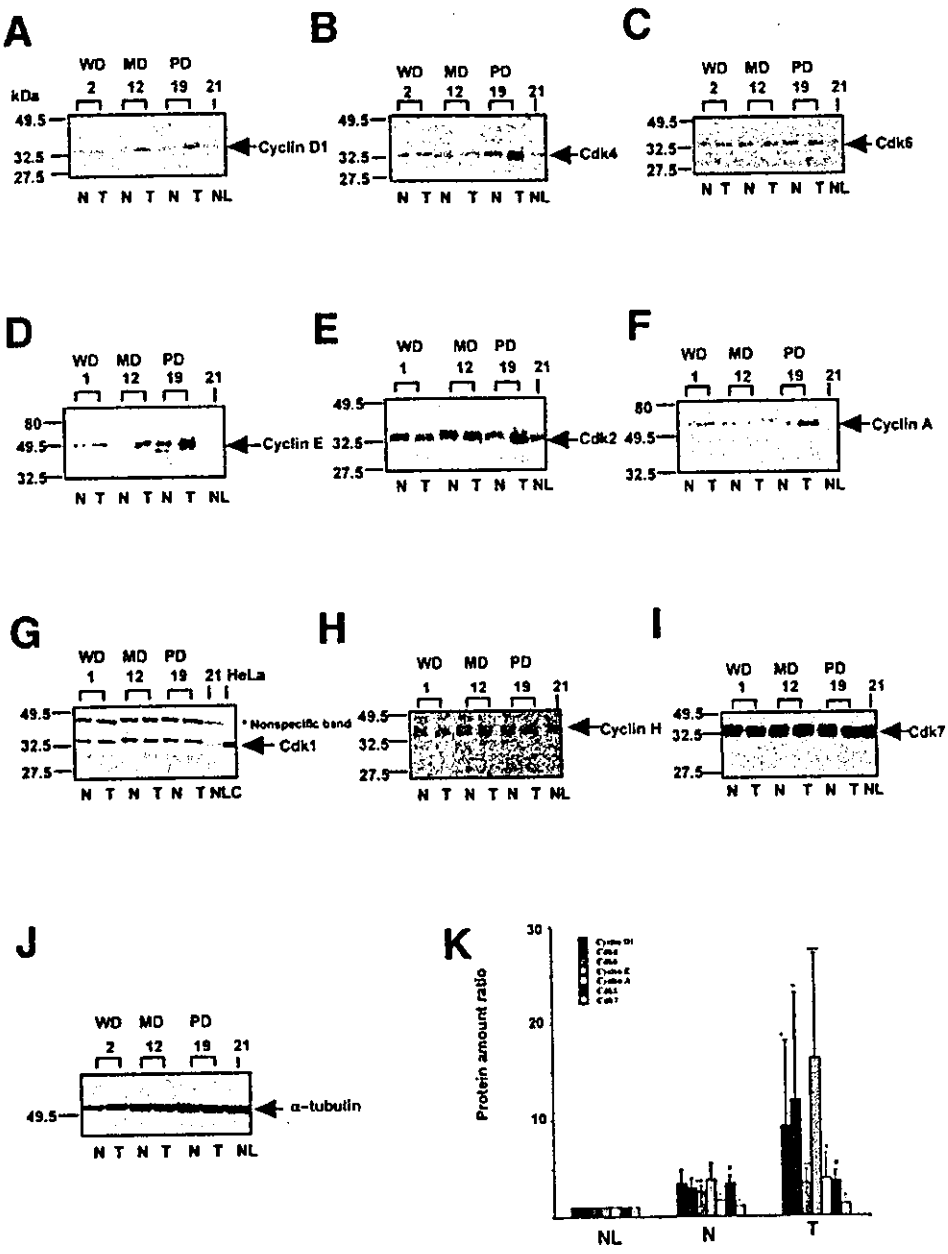

Fig. 2. Western blot of cyclin D1 (A), Cdk4 (B), Cdk6 (C), cyclin E (D), Cdk2 (E), cyclin A (F), Cdk1 (G), cyclin H (H), Cdk7 (I), and β-tublin (J) in representative nontumorous cirrhotic (N) and tumorous (T) portions of HCC and in normal liver (NL). (A-C) The 32-kd and 34-kd immunoreactive bands detected using cyclin D1 and Cdk4 antibodies (**arrows**) were seen in N and T portions, respectively. More intense immunoreactive cyclin D1 and Cdk4 bands were seen in poorly differentiated (PD) HCC than in well- (WD) and moderately differentiated (MD) HCCs. In contrast, the intensity of the 36-kd immunoreactive band for Cdk 6 was about the same in N and T tissues, irrespective of tumor differentiation. The bands for cyclin D1, Cdk4, and Cdk6 in NL were very faint. (D-F) A high level of immunoreactive cyclin E and cyclin A band (**arrow**) was seen in MD and PD HCCs, but the amount of their catalytic subunit, Cdk2, was about the same in NL, N, and T tissues (**arrow**). (G) The arrow indicates the 32-kd band corresponding to Cdk1 judging from a positive control using the HeLa cancer cell line. Although the protein level of Cdk1 was about the same in N and T tissues, it was present at only a very low level in normal liver. (H and I) The protein level of cyclin H and Cdk7 was about the same in NL, N, and T tissues of HCC. (J) The α-tubulin band represents an internal control for the amount of protein loaded. Note that the amount of α-tubulin in each lane was almost the same. (K) Levels of cell cycle-related proteins relative to the levels in normal livers as the reference levels (= 1). Values shown represent the mean ± SEM of each cell cycle-related protein for each tissue group. $P < .05$ and $P < .005$ versus N and NL tissues, respectively. $^{**}P < .01$, $P < .0001$ versus NL.

the degree of tumor differentiation. The level of the various cell cycle–related proteins in relation to the grade of HCC differentiation was generally in accordance with the level of the corresponding proteins (Fig. 5B).

The activities of cyclin D1, Cdk4, and cyclin E increased with the size of the HCC. These activities were significantly higher in HCC over 30 mm in size than in smaller HCC. In addition, strong up-regulation of cyclin

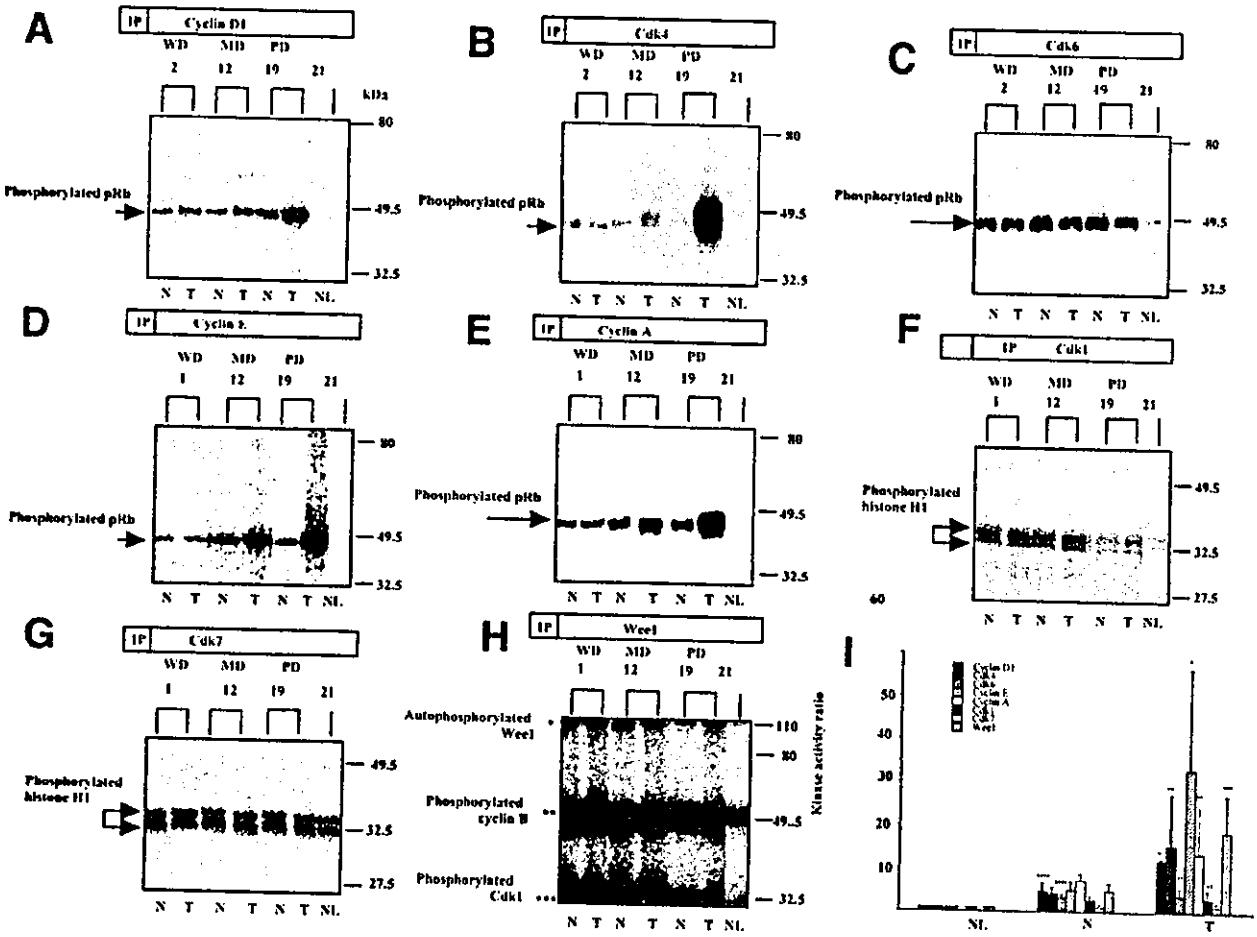

Fig. 3. Cyclin D1 (A), Cdk4 (B), Cdk6 (C), cyclin E (D), cyclin A (E), Cdk1 (F), Cdk7 (G), and Wee1 (I) kinase assays in representative nontumorous (N) and tumorous (T) portions of HCC, and in normal liver (NL). (A-E) Radioactivity in the pRb band is shown (**arrow**). Note that higher kinase activity of cyclin D1, cyclin E, Cdk4, and cyclin A was detected in moderately differentiated (MD) and poorly differentiated (PD) HCCs compared with well-differentiated (WD) HCC, whereas the Cdk6 activity was about the same in N and T tissues, irrespective of tumor differentiation. In contrast, the kinase activity of cyclin D1, Cdk4, Cdk6, cyclin E, and cyclin A was very low in normal liver. (F and G) Radioactivity in the histone H1 band is shown (**arrows**). (F) The Cdk1 kinase activity was about the same in N and T tissues irrespective of tumor differentiation, whereas the activity in NL was very low. (G) The Cdk7 activity was about the same in NL, N, and T tissues. (H) The Wee1 kinase activity using cyclin B/Cdk1 as a substrate. The upper phosphorylated protein (*) is autophosphorylated Wee1, the middle band is phosphorylated cyclin B (**), and the lower protein is phosphorylated Cdk1 (***). Note that high levels of kinase activity were detected in HCC, irrespective of tumor differentiation. (I) Relative levels of cell cycle-related kinase activities in NL, N, and T. The activity level in normal livers was used as the reference level (= 1). Values shown represent the mean ± SEM of each cell cycle-related kinase activity for each group. $P < .05$, $P < .005$, $P < .001$, and $P < .0001$, $P < .05$ versus N and NL tissues, respectively. $P < .005$, $P < .05$, and $P < .005$ versus NL.

D1, Cdk4, and cyclin E activities was detected in advanced HCC and in HCC of TNM stages III and IV (Fig. 6A). The levels of the various cell cycle–related kinase activities in stages I and II and stages III and IV were in accordance with the levels of the corresponding proteins (Fig. 6B).

Discussion

In this study, cyclin D1–related kinase activity was markedly enhanced in a subset of HCCs, especially in poorly differentiated and advanced HCCs (stages III and IV), suggesting that aberrant expression of cyclin D1–related kinase may reflect the aggressiveness of HCC and be related to tumor cell differentiation (Figs. 5A and 6A). These data appear to be consistent with the results of previous studies showing amplification and overexpression of cyclin D1 in advanced HCC.[2,3]

Cyclin D1 activates Cdk4 and Cdk6 in fibroblast cells, and thereby drives the cells through START (Fig. 1). The cyclin D1–related kinase activities can be expressed as the sum of cyclin D1/Cdk4 and cyclin D1/Cdk6 kinase activities. In this study, the Cdk4 activity in poorly differentiated HCCs was higher than that in nontumorous cirrhotic tissues, whereas the kinase activity of Cdk6 was about the same in nontumorous cirrhotic tissues and HCC (Fig. 3B, C, and I), suggesting that an increase of